THE IONIZATION PRODUCED IN NUCLEAR EMULSION BY VERY RELATIVISTIC PARTICLES

HARLAN D. HANSON
WILLIAM R. SENG
RUSSELL H. WEIDMAN

THE IONIZATION PRODUCED IN NUCLEAR EMULSION BY VERY RELATIVISTIC PARTICLES

By

Harlan D. Hanson

Lieutenant, United States Coast Guard

William R. Seng

Lieutenant, United States Navy

and

Russell H. Weidman

Lieutenant, United States Navy

Submitted in partial fulfillment of

the requirement for the degree of

MASTER OF SCIENCE

IN

PHYSICS

United States Naval Postgraduate School

Monterey, California

1 9 6 4

S ARCHIVE
04
NSON, H

THE IONIZATION PRODUCED IN NUCLEAR EMULSION BY VERY RELATIVISTIC PARTICLES

* * * * *

Harlan D. Hanson

William R. Seng

and

Russell H. Weidman

THE IONIZATION PRODUCED IN NUCLEAR EMULSION BY VERY RELATIVISTIC PARTICLES

By

Harlan D. Hanson

William R. Seng

and

Russell H. Weidman

This work is accepted as fulfilling

the thesis requirements for the degree of

MASTER OF SCIENCE

IN

PHYSICS

from the

United States Naval Postgraduate School

ABSTRACT

In order to determine the shape of the ionization curve in nuclear emulsions at values of $\tau > 100$, we have measured the blob density of relativistic electron tracks. The pv of the pair produced electrons used was determined by multiple scattering. A total of 84.45 centimeters of electron track was blob counted and scattered. From $\tau = 100$ to $\tau = 5400$ the data were combined into 14 points each with a statistical uncertainty on blob density of less than 1%. These points indicate a level "plateau" and show no deviation from this plateau within our statistical accuracy. Pions were used to estimate the minimum of the ionization curve, and ratio of blob density plateau to blob density minimum is estimated to be $1.140 \pm .020$.

TABLE OF CONTENTS

LIST OF ILLUSTRATIONS

1. Introduction

The classical theory of the energy loss of a charged particle passing through matter was developed by Bohr /1/ and later extended quantum mechanically by Bethe /2/ and Bloch /3/. These theories predicted that the energy loss by ionization per unit path length was a function of velocity and charge. In particular the energy loss was to decrease approximately as $1/v^2$ to a minimum at $v/c \simeq 0.96$. After this minimum the energy loss should logarithimically increase indefinitely due to relativistic effects on the electric field of the charged particle. Swann/4/ predicted, however, that the increase in energy loss would be limited, in condensed substances, by the polarization of the medium. Quantitative calculations by Fermi /5/, treating the electrons in the medium as classic oscillators of one frequency, showed that the most probable energy-loss per unit path length should increase to and remain at some maximum value which depends on the density of the medium. This maximum value was therefore called the "Fermi Plateau", and the polarization effect the "density effect." Fermi's theory has been extended and elaborated upon, using multi-frequency theory, by Wick /6/, Halpern and Hall /7/, Schönberg /8/, and Sternheimer /9/; but these extensions show no significant difference at $v \simeq c$ and also predict a "plateau." Although emulsion groups were eager to measure the relativistic and density effects in solid media, it was not until 1948 that

Berriman introduced photographic emulsions that were sensitive to singly charged particles of minimum ionization.

The first attempts to measure the relativistic rise met with negative results. These early experiments are discussed by Price /10/. However, in 1950 Pickup and Voyvodic /11/ reported the first experimental indications of a relativistic rise. Corson and Keck /12/, McDiarmid /13/, and Morrish /14/ reported the existence of an ionization plateau; but none of these experiments carried their measurements down to the ionization minimum. Two more experiments published in 1952 showed a relativistic increase in grain density from minimum to plateau, but differed in the magnitude. Daniels et al /15/ reported a rise of about 8%, while Shapiro and Stiller /16/ obtained an experimental ratio of $1.12^{+0.04}_{-0.03}$. Stiller and Shapiro /17/ duplicated their experiment the following year using blob count instead of grain count as a measure of ionization and found virtually the same results--a saturation of the curve at $\gamma > 100$, and a rise above minimum of about 14%. Michaelis and Violet /18/ and Fleming and Lord /19/ also attempted to measure the ratio of ionization at plateau to ionization at minimum. In both experiments two points were plotted: one near minimum and one near plateau. These experiments have, underlying their design, the implicit assumption of a constant Fermi plateau. Experimenters were now trying to measure two parameters: at what value of γ the "plateau"

begins, and how far above the ionization minimum the "plateau" lies. The results of Alexander and Johnston /20/ are quoted as a value of grain density plateau/grain density minimum of $1.133 \pm .008$, and Jongejans /21/ has stated in 1960:

> It seems that a remarkable agreement exists about the ratio plateau to minimum; we find
>
> $$\frac{g_p}{g_m} = 1.129 \pm .010$$
>
> This value compared with 1.133 ± 0.008 of Alexander and 1.14 ± 0.03 of Stiller.

Recently an extensive study of the relativistic rise of grain density was carried out by Patrick and Barkas /22/, but their main attention was focused on the rise from minimum and transition to plateau.

Theoretical studies /23-26/ were continuing, but the major effort was devoted to finding the exact shape of the curve in the interval during the relativistic rise and transition to plateau. If the ionization curve could be plotted accurately in this range of γ, the identification of particles with velocities in this range could be made. The rate of energy loss per unit path could be measured; and together with a measurement of velocity, would give the particle identity even on tracks which passed from the emulsions. It is not surprising that the plateau region was given relatively little attention. Price /10/ perhaps best sums up the prevailing feeling when he says:

> This is a field of work in which the theory was largely established well before any experimental verification was possible, and in which spectacular discoveries were neither expected nor obtained.

In 1962, however, Alekseyeva et al /27/ reported such a discovery. They announced that their theory predicts instead of a flat plateau, a decrease of the ionization loss at very high velocities. Furthermore, they stated that their experimental work was in agreement with their theory. Their data show a drop of several per cent in the blob density of electrons in the region between $\gamma \simeq 200$ and $\gamma \simeq 600$ $(\gamma = 1/\sqrt{1 - v^2/c^2})$. In work done at the same time, the data of Stiller /28/ show a slight tendency to "peak" at $\gamma \simeq 750$. Since previous data above $\gamma \simeq 200$ had a statistical accuracy no better than 2%, earlier experiments were able neither to confirm nor to refute the Russian theory. With these facts in mind, we decided to attempt the task of gathering sufficient data to provide a statistical accuracy of 1% at high values of γ. Since the area of high γ had previously been neglected, we decided to concentrate our efforts in this area and to take only enough data below $\gamma = 100$ to establish the fact that our measurements were sensitive enough to detect any variation in the curve. The precise details of the formulation of the experiment are given in the next section.

We have multiple scattered a total electron track length of 84.45 centimeters and counted 191,195 electron blobs. We find

no significant evidence for a departure from a flat "plateau" in the region $\gamma > 100$.

2. Formulation of the Experiment

After the purpose of this experiment had been decided, it was necessary to formulate our exact procedures. Since we wanted to measure particles with γ as high as possible, we chose to work with electrons. One source of these high γ electrons is pair production, using the gamma rays from the decay of neutral pions for initiation of the pair production.

$$\pi^0 \xrightarrow{10^{-17}\ \text{sec}} \gamma + \gamma$$

The neutral pions are obtained from interactions of high energy primary beam particles with nuclei in the emulsion. K. I. Alekseyeva et al /27/ used this same procedure, using 19.6 Bev. protons as the primary beam particles.

The choice of primary beam particles was made with two criteria in mind. First, the beam energy should be as high as possible, since the number of neutral pions formed in the primary star (and hence the number of pair produced electrons) is a function of the beam energy. Second, Shapiro /29/ indicates that the particles used for normalization should have $\gamma > 100$. To satisfy these two conditions, pellicles were used that had an incoming π^- beam of 16.2 ± 0.6 Bev. This corresponds to $\gamma \cong 115$ and enabled us to use the primary beam particles as our normalization particles. Because of the source of electrons, an area one centimeter square located seven centimeters from the primary

beam entrance end was chosen. This area was then scanned for electron pairs. There were 42 electron pairs found in pellicle $\mathcal{R}$ -132, 67 in pellicle $\mathcal{R}$ -133, and 72 in pellicle $\mathcal{R}$ -134.

The pellicles we used were from a 600 micron Ilford K-5 emulsion stack which was exposed to a 16.2 $\pm$.6 Bev π^- beam at CERN in 1960. This stack was flown to Berkeley, California, and developed there four days after exposure. Of the 180 pellicles in the stack, numbers 121 through 180 are at the United States Naval Postgraduate School on loan from Dr. Walter H. Barkas at Lawrence Radiation Laboratory.

Although it would have been desirable to measure the rate of ionization loss over the entire energy range with a single species of particle, electrons of energy less than 30 Mev are difficult to measure. This difficulty arises largely because at these energies, electrons suffer large multiple scatterings. Because of the strong scattering: (1) it is difficult to contain the electron in an emulsion for any significant length; (2) the probability of inadvertantly shifting to another track is high; (3) it is difficult to separate the background count from the true count; and (4) the measurement of the electron track length becomes somewhat subjective. We therefore used pions and protons from the primary stars as our source of data for $\gamma < 40$. Although it was not our intention to measure accurately the details of the rise to plateau, we wanted to be sure that our measurements were sensitive

enough to detect a rise.

In order to calculate the pv values of the electrons, protons, and pions, a program was written for the CDC 1604 computer at the USNPGS. A discussion of this program, along with the program flow chart and printout are included in the appendices. Three physicists did the multiple scattering on each track, scattering each electron track at least twice to prevent misidentification. For fast electrons the determination of pv is complicated by the radiative energy loss along the electron path. In order to minimize errors resulting from this effect, no single electron track was scattered for more than 1.5 centimeters, and most were scattered for only 0.5 centimeters. Each computer program output was analyzed for bremsstrahlung effects (see appendices), and if a bremsstrahlung was suspected, the track was discarded. Furthermore, the same segment of electron track used in the measurement of pv was used in the measurement of blob density. Thus if some undetected bremsstrahlung did occur along the electron track, the blob density and the value of γ would be averaged over the same range of pv.

As a measure of the rate of ionization loss, we have used blob density rather than grain density. The greater information content of other track parameters /22, 26/ is offset for near-minimum tracks by the ease and accuracy with which blob density data can be gathered. Accuracy in this sense means reproducibility. Price /10/ has stated that it is possible to obtain

results by blob counting that vary by no more than 0.5% between observers.

Although the rise from minimum to "plateau" might have been different had we used grain density, the shape of the "plateau" should not change. That is, if a drop from "plateau" exists when grain density is used as a measure of ionization, it will also exist when blob density is used. Therefore, all data in this paper is presented in terms of blob density.

Two scanners were given the task of blob counting all tracks used. To prevent the need for calibration between the two scanners, each had two pellicles of her own. All blob counting in each pellicle was thus done by one observer. The electron and pion tracks were normalized to tracks of the primary pion beam at the same depth in the emulsion. Periodic recounting of random tracks showed that several months were required to reach a satisfactory reproducibility of 1%. Because of this effect, much of the data gathered in the early part of this experiment were eventually discarded. The data presented in this paper are from three pellicles. Additional data from the fourth pellicle will be published at a later date.

3. Measurement of particle velocities

Multiple scattering measurements were made on each track to estimate the product of momentum and velocity, pv. The velocity and the corresponding value for τ were then calculated. Scattering measurements were performed on proton, electron, and pion tracks using a Koristka R-4 microscope. The calculations were accomplished on a CDC 1604 computer; a program description, flow chart, and listing for which are included in the appendices.

The same basic computation was used to estimate the value of pv for all particles. The expression /30/;

$$pv = \frac{K_{co}\ (s)^{3/2}}{573\ D} \qquad \text{(in Mev.)}$$

was used for calculations. The scattering constant, K_{co}, is that appropriate for a cut-off without replacement at four times the true mean second difference, D. The cell length, s, is in microns.

The scattering constant was evaluated from the expression;

$$k_{co}^2 = 675\,[0.090 + 0.272\,\mathrm{Log}_{10}(5s')]$$

where the constants are those given by Scott /31/ and adjusted by Barkas /30/. The equivalent cell length, s', corrects for the dependence of K_{co} on particle velocity and charge. The same references supply the expression for the equivalent cell length;

$$s = (0.23 + 0.77\ v^2/c^2)(s')$$

for singly charged particles.

Noise was removed from the scattering measurements for each track by two distinct procedures. The methods used were: (1) cell length variation /32,30/ using cell lengths of one, two, and three times the prime cell length, and (2) subtraction of a constant noise appropriate to each observer.

Using cell length variation the noise can be estimated from:

$$\text{Noise squared } (i,j) = {}_i\overline{\Delta}^2 - \left[\frac{{}_j\overline{\Delta}^2 - {}_i\overline{\Delta}^2}{\left(\frac{j}{i}\right)^{3+0.14} - 1}\right]$$

In this expression ${}_i\overline{\Delta}$ and ${}_j\overline{\Delta}$ are the means of the absolute values of the measured second differences using cell lenghts of i and j times s. The indices i and j vary from one to three; however $i \neq j$. The factor of 0.14 in the exponent comes from considering the scattering constant as a function of cell length. The noise was calculated using cell overlap combinations of (1,3), (1,2), and (2,3) times the prime cell length. The three values were compared for consistency but the value of noise using cell overlap of (1,2) was the only one used in estimating the true signal.

Repeated scattering measurements were performed on the 16 Bev primary pions by all observers. For pions of this energy, apparent scattering is almost completely noise. Using this noise, q, the true mean second difference for an electron track

was estimated from:

$$D^2 = \overline{\Delta}^2 - q^2$$

where $\overline{\Delta}$ is the measured total mean second difference. Prime cell lengths of 100, 250, and 500 microns were used with the resultant noise found to be nearly independent of these cell lengths.

All tracks were scattered twice, usually by different observers. Tracks which did not yield results in statistical agreement, either between observers or method of noise removal, were discarded or rescattered.

For fast electrons, the determination of pv is complicated by the radiative energy loss along the path of the electron. To minimize this, no electron track was scattered more than 1.5 cm. Further, any electron track which showed evidence of a change in pv along the scattered length, either as a noticeable single scatter or as indicated by the computer program, was discarded. The computer divides each track into segments ten cell lengths long to facilitate the detection of changes in pv possibly caused by bremsstrahlung. (See app. I)

Of a total of 362 electron tracks (181 pairs) located in the scanned areas of the three plates, 225 were discarded because of detectable bremsstrahlung or because the length of track in one pellicle did not allow a minimum of 20 prime cell lengths.

In addition to scattering each track twice, requiring agree-

ment between methods in determination of D, and requiring that no detectable bremsstrahlung occur in the used portion of the track; all tracks used met the conditions shown in Fig. 1.

	Min. sig/n	Min No. of S	S used (micron)	Optimum No. of S
$pv \leq 200$	1.5	20	100	40
$200 < pv \leq 1000$	1.5	20	250	40
$pv > 1000$	1.5	20	500	30

Fig. 1 Useability Criteria

Fig. 3 /33/ was used to estimate the minimum cell length to use for scattering to expect a signal to noise ratio $\geq$ 1.5 for a specific value of pv.

The standard deviation, σ, of pv determinations was estimated using $\sigma = \frac{137}{\sqrt{f n \lambda}}$ /32/; where n is the number of prime cells, λ is the degree of overlap, and f is taken from Fig. 2.

λ	1	2	3
f	1	1.022	1.046

Fig. 2 Overlap Form Factors

Using the criteria in this section, the estimated errors in pv ranged from 15 to 30 percent.

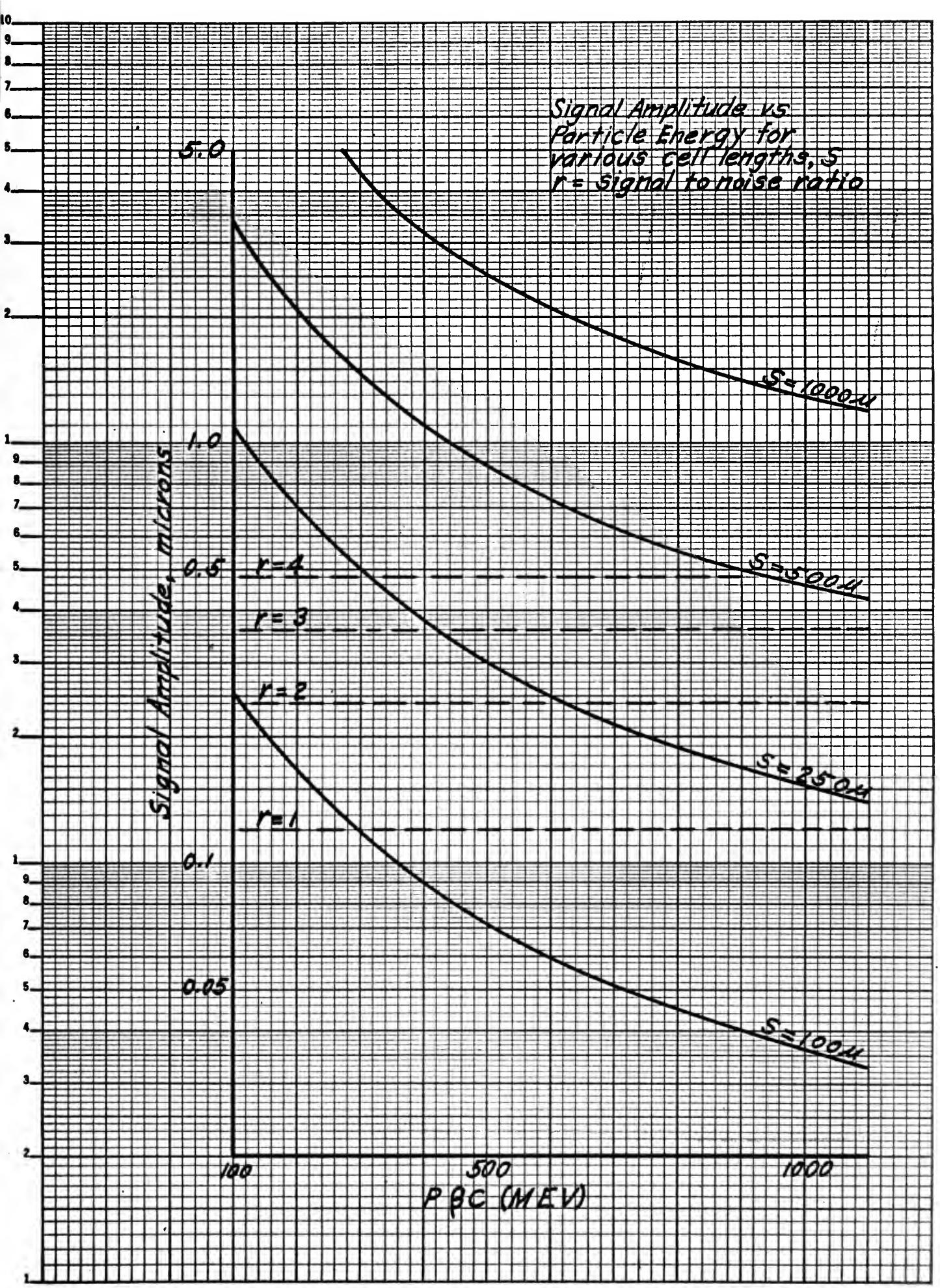
Signal Amplitude vs.
Particle Energy for
various cell lengths, S
r = signal to noise ratio
5.0
1.0
0.5
0.1
0.05
r=4
r=3
r=2
r=1
S=1000μ
S=500μ
S=250μ
S=100μ
Signal Amplitude, microns
100
500
1000
PBC (MEV)

FIG. 5

4. Measurement of ionization

Blob density has been used as the measure of ionization in this experiment. The greater information content of other track parameters, such as grain density or mean gap length /34/, is offset for near minimum tracks by the ease and accuracy with which blob density data can be gathered. Bausch and Lomb microscopes, with magnification of about 16 x 100, equipped with coordinate stages by the Lawrence Radiation Laboratory at Berkeley, California, were used for blob counting.

The energy of fast electrons decreases exponentially with increasing track length in the emulsion. As the blob density is also a function of energy, care was taken to assure the scattering measurements for second differences and the average blob densities were obtained over the same portion and length of each electron track. Therefore if some undetected radiative energy loss occurred along an electron track, the ionization loss and the value of γ are averaged over the same range of pv.

Blob count calibration curves for the three plates used are shown in Fig. 4. These curves describe the variation of blob density with depth in the emulsion for each of the pellicles. To obtain these plots, the pellicle thickness was divided into tenths and then the blob density of the primary pions within each tenth of pellicle thickness was determined. Each point represents about 12 tracks or 5,000 blobs. These tracks were all located

in the same region as the electron pairs. The variation in these curves for pellicles processed together, clearly shows the need for careful calibration of each pellicle. (See subhead 7, Critique)

All blob density data were collected by two scanners. All counting in a given plate was done by one. Both scanners were required to return periodically to their "normalization tracks" (primary pions) to check for any change in subjective criteria used in blob counting. Changes did occur, and much of the data gathered in the early part of the experiment had to be discarded because of this. Several months were required to reach reproducibility of about one percent. It should be noted the two scanners had a continued systematic difference of about 3% in their counts of the same tracks. As a consistency check the shape of one of the curves of Fig. 4, that for Я-134, was reproduced by each scanner.

The electron and pion blob densities were normalized by forming the ratio of blob density of a track to that of the primary pions at the same depth in the emulsion. To select the primary pion blob density to be used for normalizing a given track, the initial and final depths in the emulsion for that portion of the track used in data gathering were determined. The calibration curves were considered as linear sections and a weighted average track depth was used to establish the depth in the emulsion of the primary pion to be used for normalization.

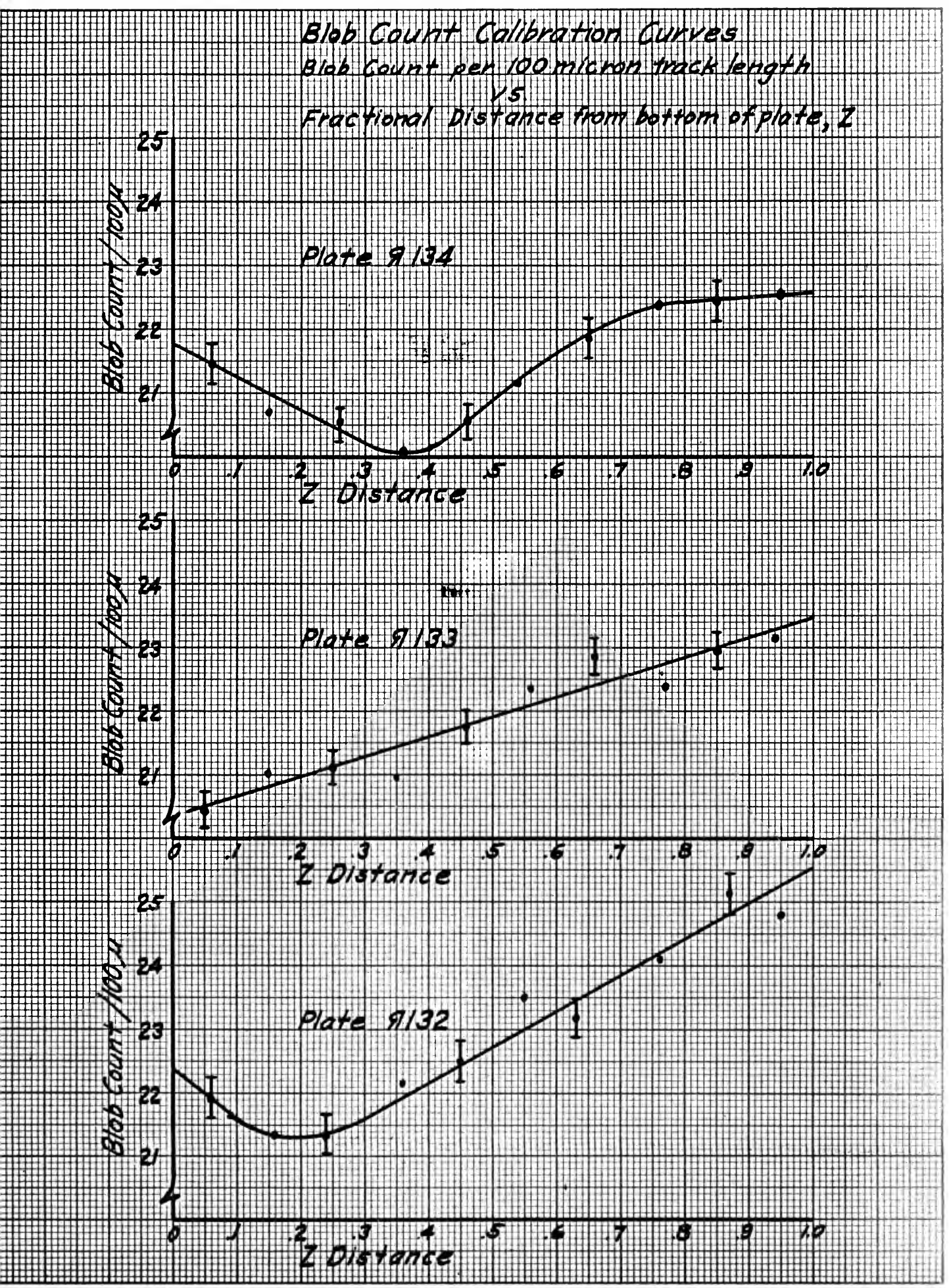
Blob Count Calibration Curves
Blob Count per 100 micron track length
vs.
Fractional Distance from bottom of plate, Z
Plate 9134
Plate 9133
Plate 9132
Blob Count/100μ
Z Distance
25
24
23
22
21
0
.1
.2
.3
.4
.5
.6
.7
.8
.9
1.0

FIG. 4

5. Results

The effect which this experiment was designed to detect was a 5% variation in ionization loss at values of γ greater than 200. For γ greater than 10, data were processed to provide a statistical uncertainty on all points plotted in Fig. 12, 13, and 14 of 2% or less. At lower γ values, no statistical uncertainty exceeds 3%.

To provide this degree of certainty, several tracks were combined to produce each data point, but each point represents only one type of particle. Tracks were added together, beginning with the lowest value of γ, until the sum of the blob count, N, for each point was such that $100X\sqrt{\Sigma N}/\Sigma N = 2\%$ or 3% as described above.

Since the 16.2 BeV pions ($\gamma \simeq 115$) to which the stack was exposed have an ionization loss which differs by less than 1% from the ionization loss of the plateau, the blob count for these tracks was selected as the value to which all others should be normalized. The effect of normalization on the data for each plate is illustrated by comparing Figs. 6, 7, and 8 with Figs. 9, 10, and 11 for plate numbers 132, 133, and 134 respectively.

The following relations describe how the normalized mean blob count, $\bar{c}$, the ordinate of Figs. 12, 13, and 14, was determined for each point.

N_i = Number of blobs in the ith track

N_o = Number of blobs in the same length of 16.2 BeV pion track

m_i = Number of blobs per 100 microns of track

n_o = Number of blobs per 100 microns of 16.2 BeV pion track

$n_i = N_i/m_i$

$c_i = n_i/n_o = N_i/m_i n_o$ or $c_i = \dfrac{N_i \pm \sqrt{N_i}}{m_i n_o}$ assuming N_i has a statistical uncertainty of $\sqrt{N_i}$.

$$\sigma^2(c_i) = N_i/m_i^2 n_o^2$$

The $\bar{c}$ is the average of the c_i's weighted according to the inverse square of the statistical uncertainty. The summation is over the number of tracks involved.

$$\bar{c} = \frac{\sum \dfrac{c_i}{\sigma_i^2(c_i)}}{\sum \dfrac{1}{\sigma^2(c_i)}} = \frac{\sum \dfrac{c_i m_i^2 n_o^2}{N_i}}{\sum \dfrac{m_i^2 n_o^2}{N_i}} = \frac{\sum c_i N_i \left(\dfrac{n_o^2}{n_i^2}\right)}{\sum N_i \left(\dfrac{n_o^2}{n_i^2}\right)}$$

or $\bar{c} \simeq \dfrac{\sum c_i N_i}{\sum N_i}$ since (n_o^2/n_i^2) adjusted only the third decimal place of the normalized blob count. Therefore each track is weighted according to the number of blobs counted.

The value of Υ for a given point represents the arithmetic average of the values found for each track represented by that point. On the plateau, the maximum spread of the values represented by any given point is 22% of the value at that point.

(Fig. 14, plate 134, γ = 2600.) A typical spread is about 10%. Thus the points are separated by a distance somewhat greater than the error in γ .

These processes were used for determining the γ and normalized blob count of each point for each of the three plates, separately, to produce the curves of Figs. 12, 13, and 14. Combining these plates by superimposing the plateau regions produced the curve of Fig. 5. This method of combination was dictated by the overwhelming statistical weight associated with the information in the plateau region as compared to the information in the remainder of the curve. (For electrons, a total track length of about 84 cm. was examined.)

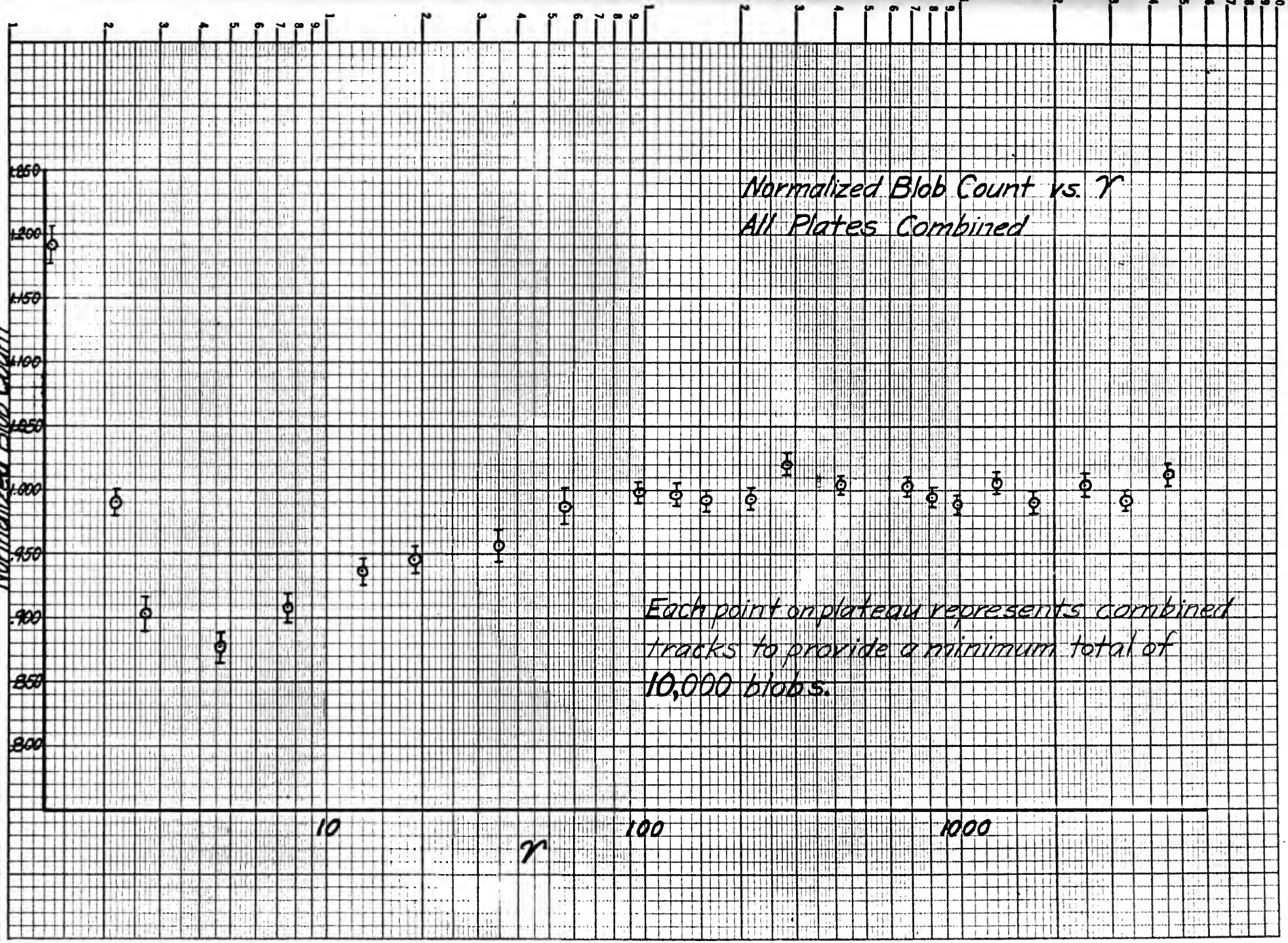
Normalized Blob Count vs. γ
All Plates Combined
Each point on plateau represents combined tracks to provide a minimum total of 10,000 blobs.
Normalized Blob Count
1.050
1.200
1.150
1.100
1.050
1.000
.950
.900
.850
.800
10
γ
100
1000

Fig. 5

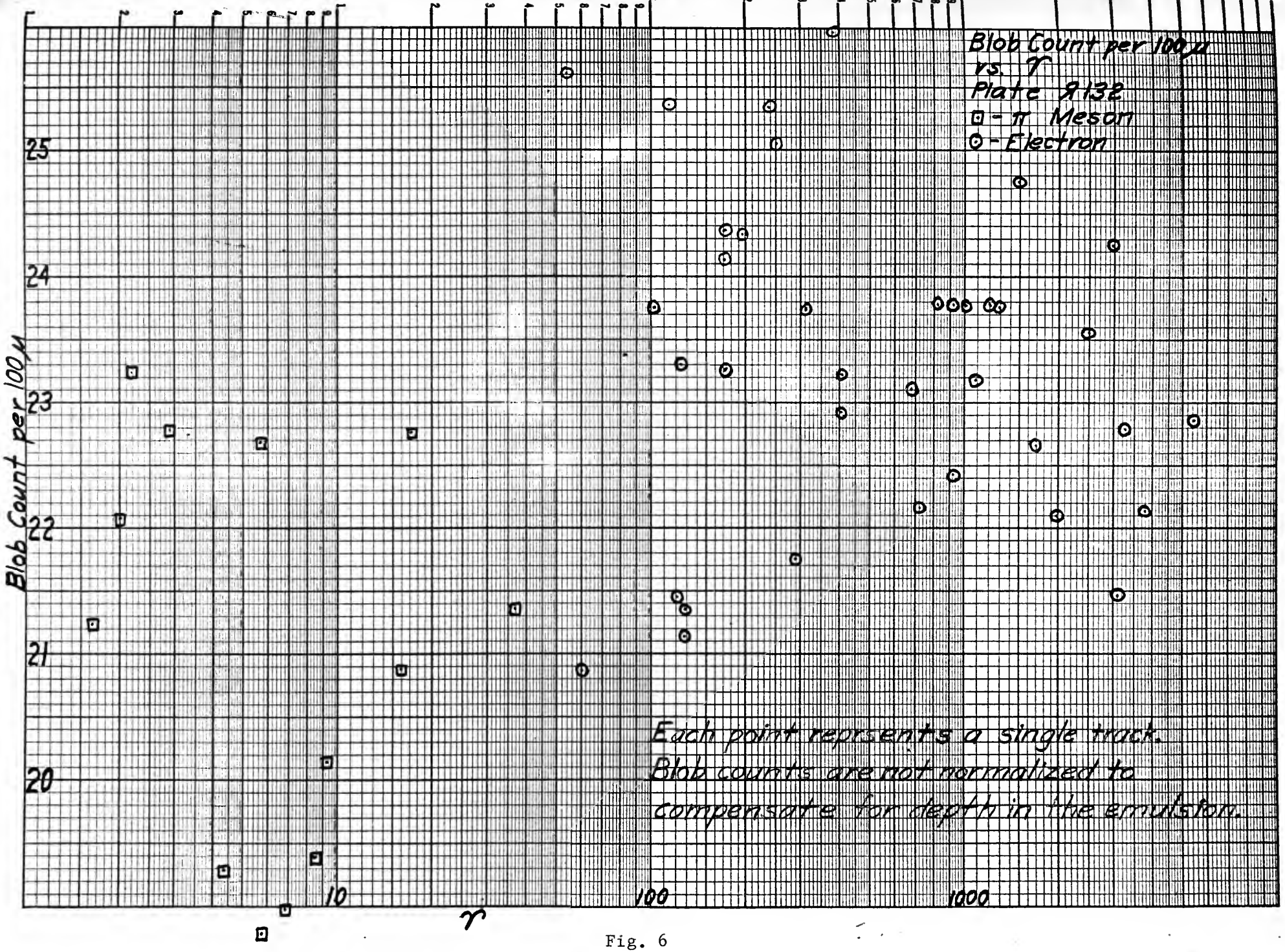
Blob Count per 100 μ
vs. γ
Plate 9132
□ - π Meson
⊙ - Electron
Blob Count per 100 μ
25
24
23
22
21
20
10
100
1000
γ
Each point represents a single track.
Blob counts are not normalized to
compensate for depth in the emulsion.

Fig. 6

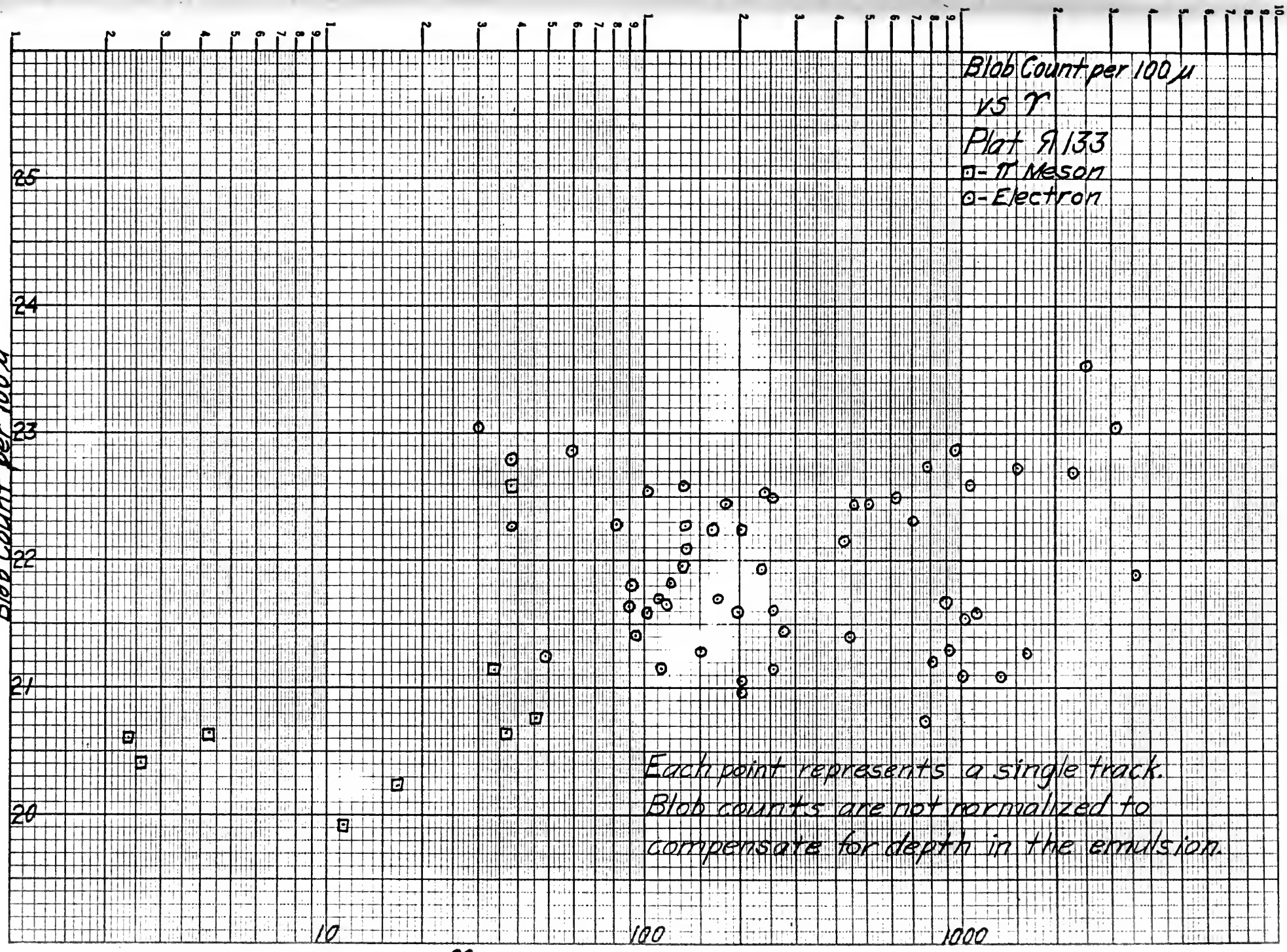
Blob Count per 100 μ
vs r
Plat 9 133
□ - π Meson
○ - Electron
Each point represents a single track.
Blob counts are not normalized to
compensate for depth in the emulsion.
Blob Count per 100 μ
25
24
23
22
21
20
10
100
1000
r

Fig. 7

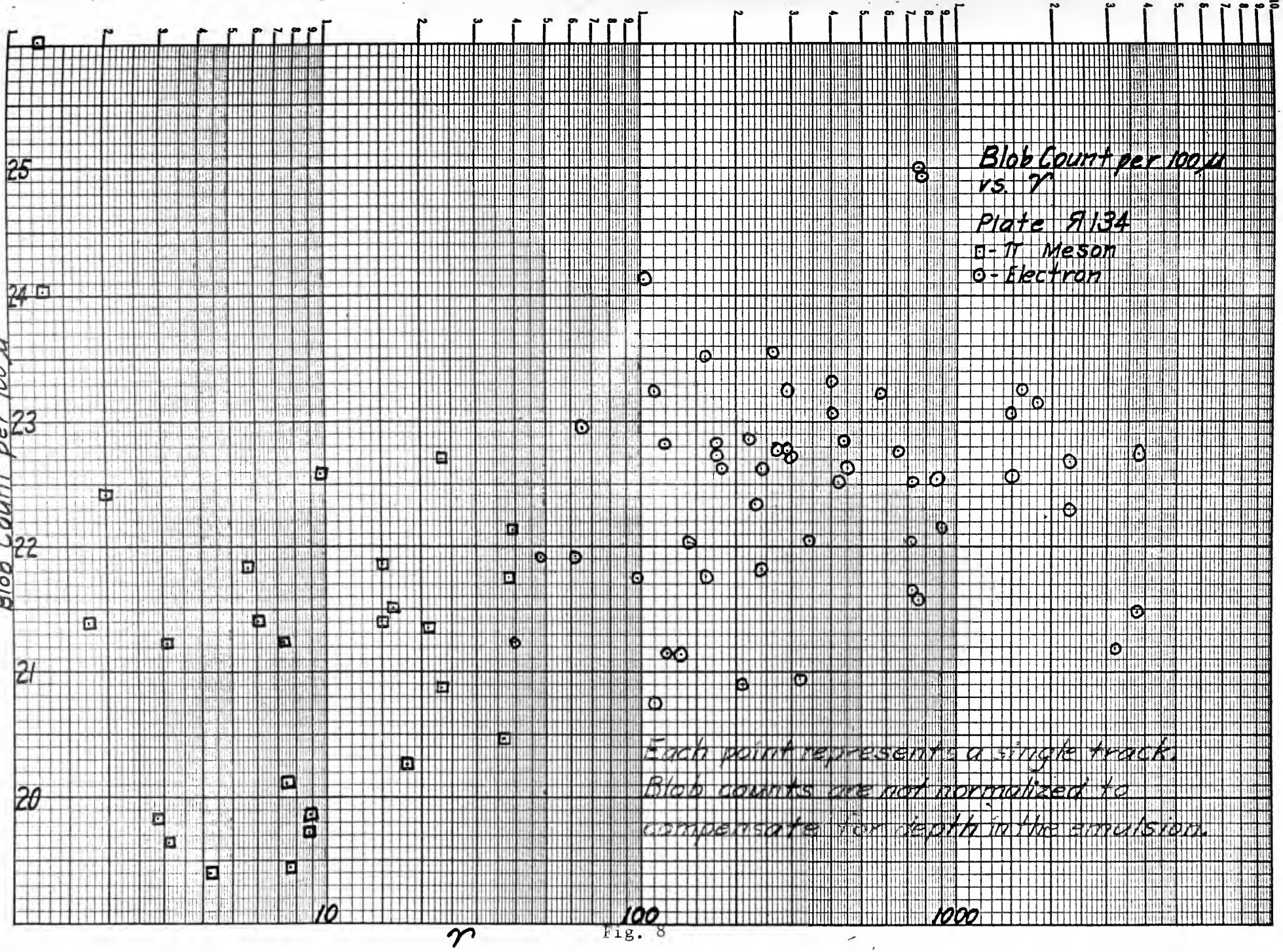
Blob Count per 100 μ vs. γ
Plate R 134
□ - π Meson
○ - Electron
Each point represents a single track. Blob counts are not normalized to compensate for depth in the emulsion.
Blob Count per 100 μ
γ
25
24
23
22
21
20
10
100
1000

Fig. 8

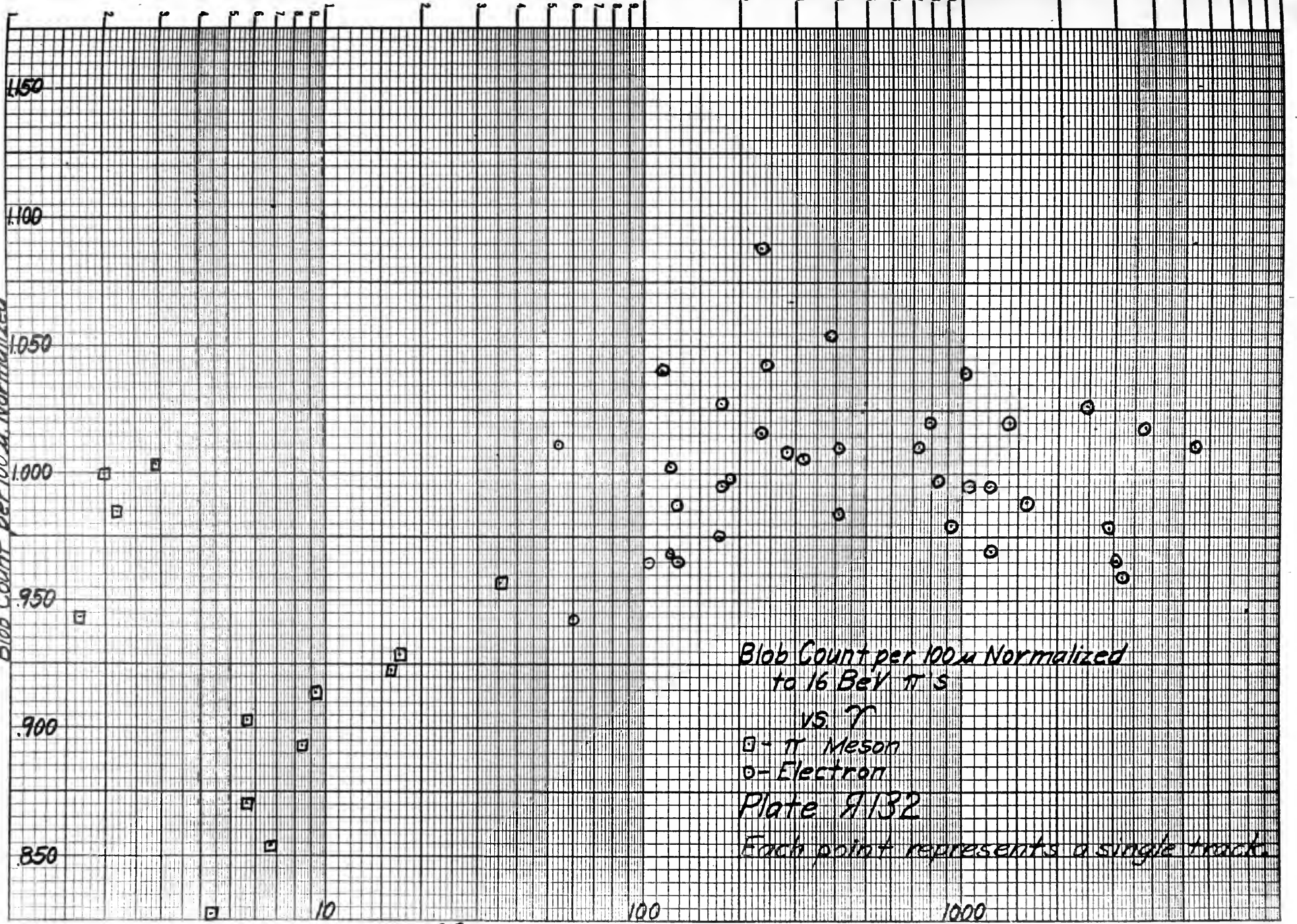
1.150
1.100
1.050
1.000
.950
.900
.850
Blob Count per 100 μ Normalized
10
100
1000
γ
Blob Count per 100 μ Normalized
to 16 BeV π's
vs. γ
□ - π Meson
○ - Electron
Plate 9132
Each point represents a single track.

Fig. 9

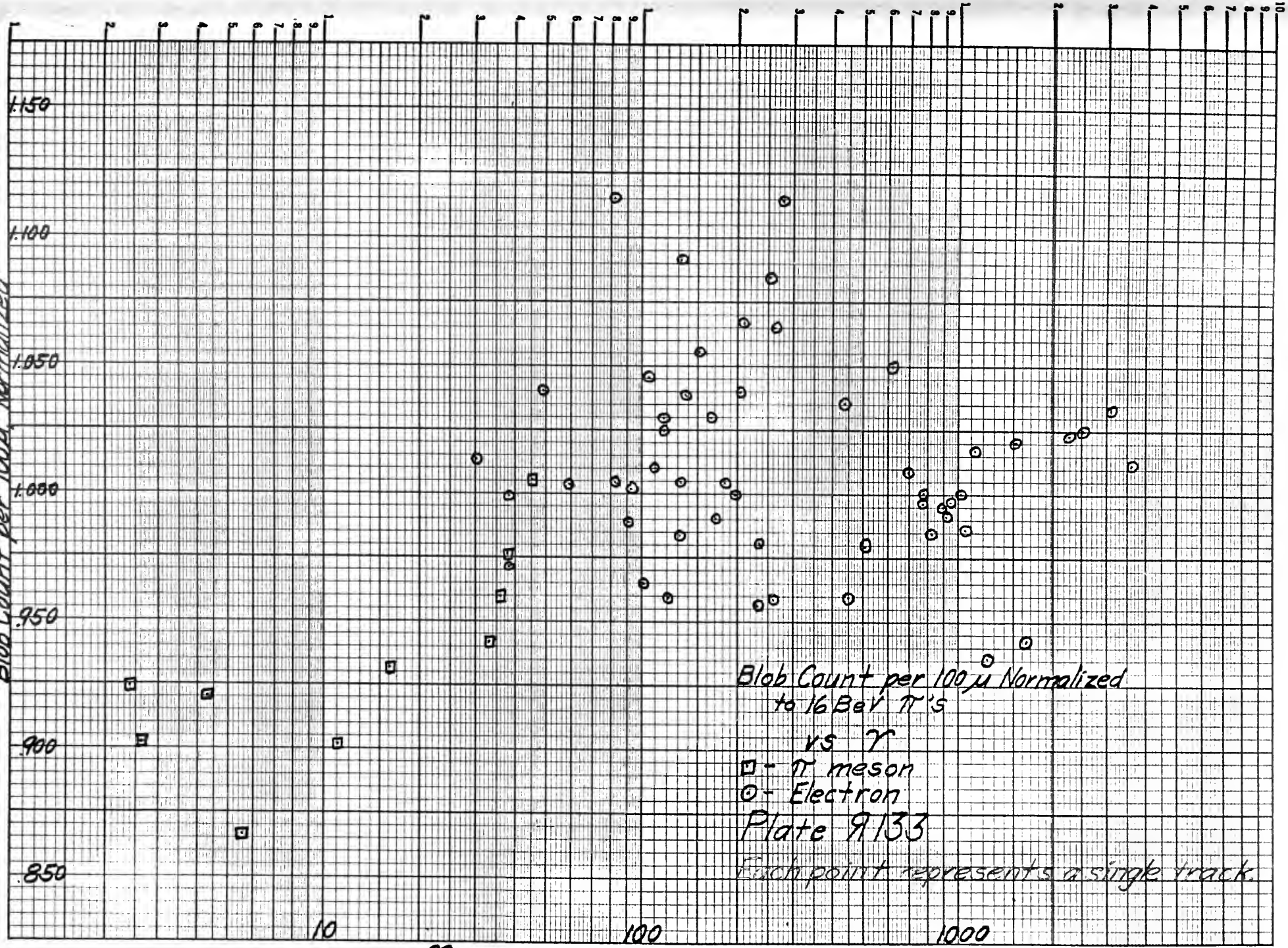
Blob Count per 100μ Normalized
1.150
1.100
1.050
1.000
.950
.900
.850
10
100
1000
γ
Blob Count per 100 μ Normalized
to 16 Bev π's
vs γ
□ - π meson
⊙ - Electron
Plate 9133
Each point represents a single track.

Fig. 10

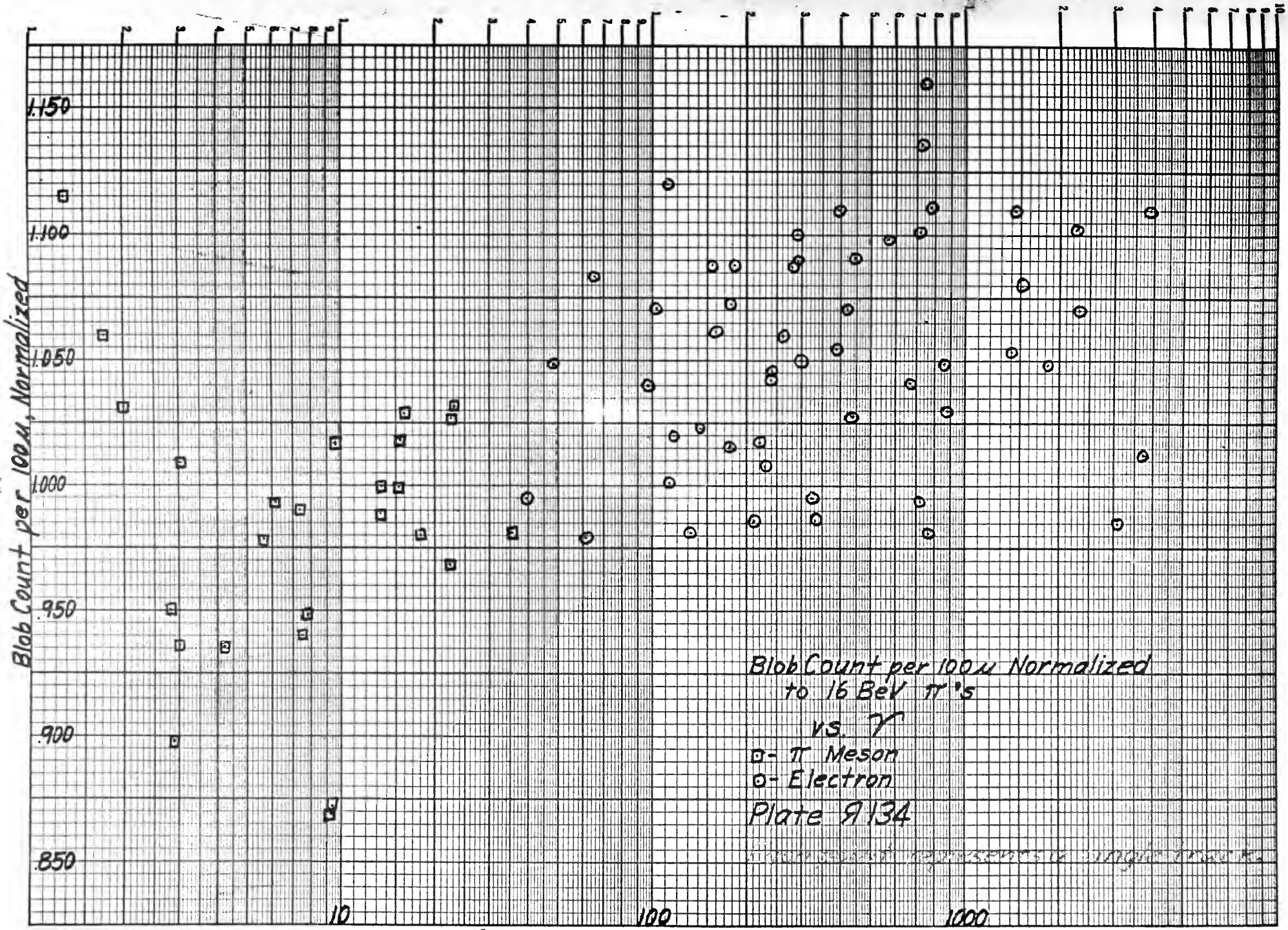
1.150
1.100
1.050
1.000
.950
.900
.850
Blob Count per 100μ, Normalized
10
100
1000
γ
Blob Count per 100μ Normalized
to 16 BeV π's
vs. γ
□- π Meson
○- Electron
Plate 9134

Fig. 11

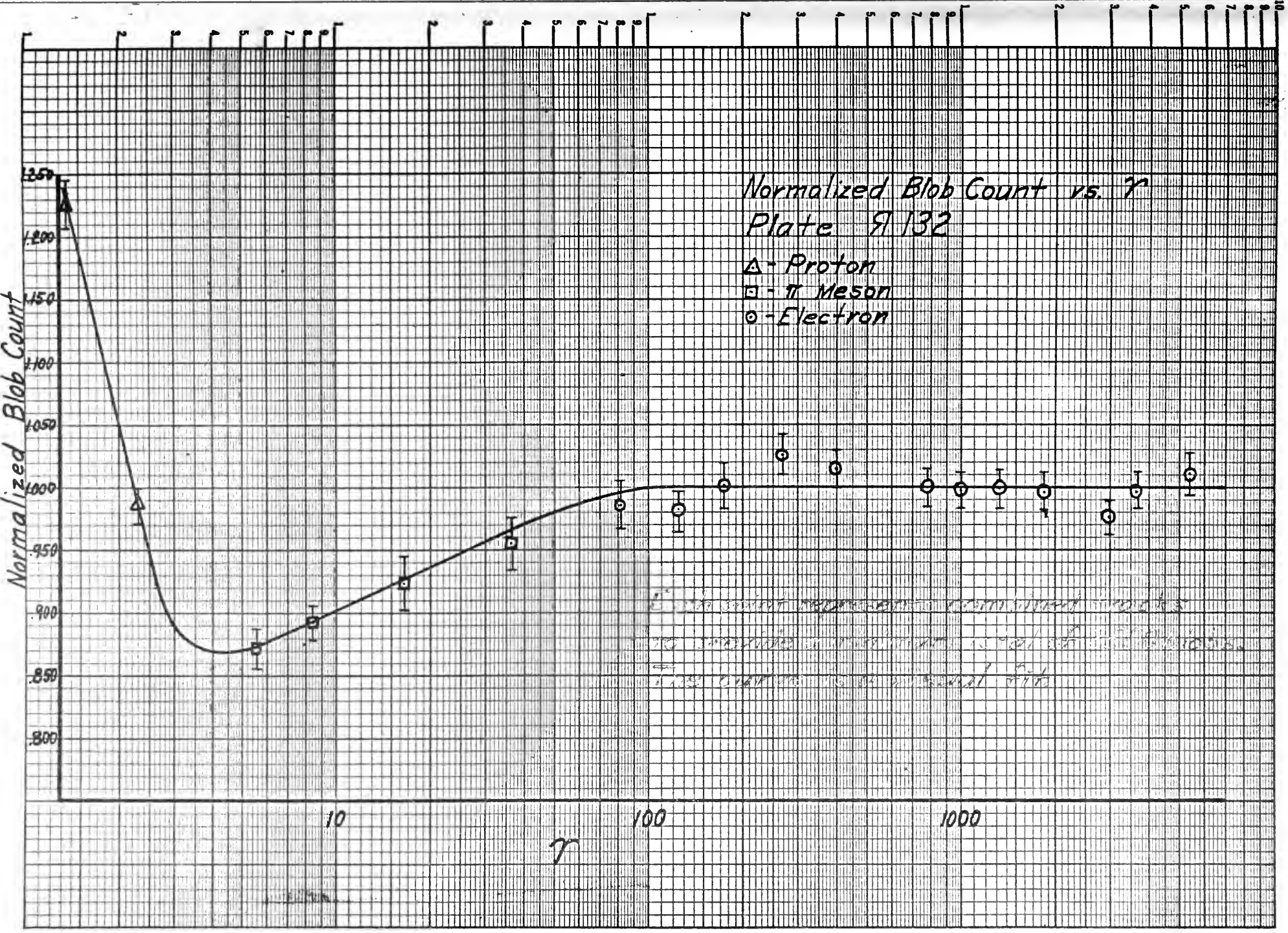
Normalized Blob Count v.s. γ
Plate Я 132
△ - Proton
□ - π Meson
⊙ - Electron
Normalized Blob Count
1.250
1.200
1.150
1.100
1.050
1.000
.950
.900
.850
.800
10
100
1000
γ

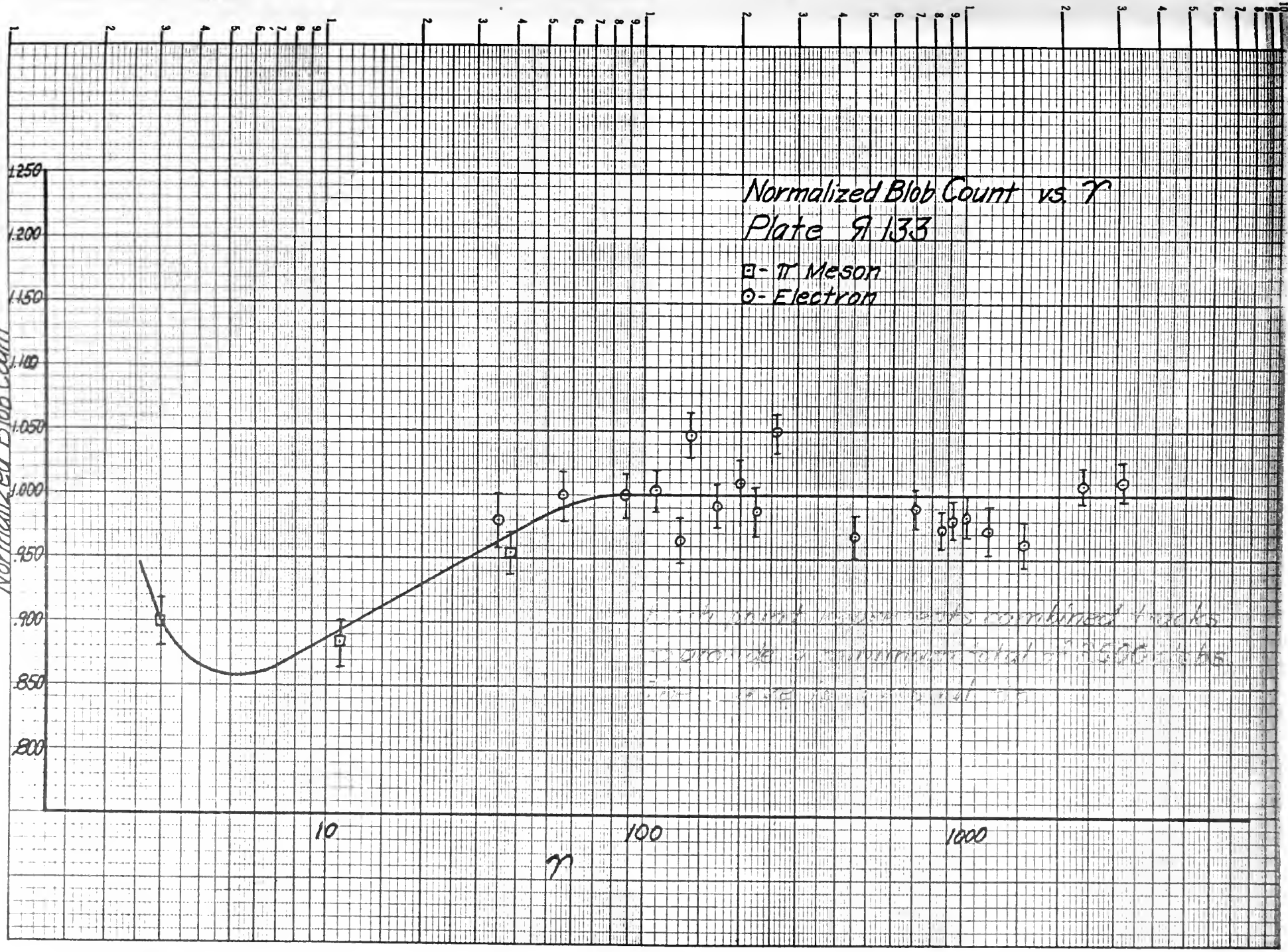
Normalized Blob Count vs. γ
Plate 9 1133
□ - π Meson
○ - Electron
Normalized Blob Count
1.250
1.200
1.150
1.100
1.050
1.000
.950
.900
.850
.800
10
100
1000
γ

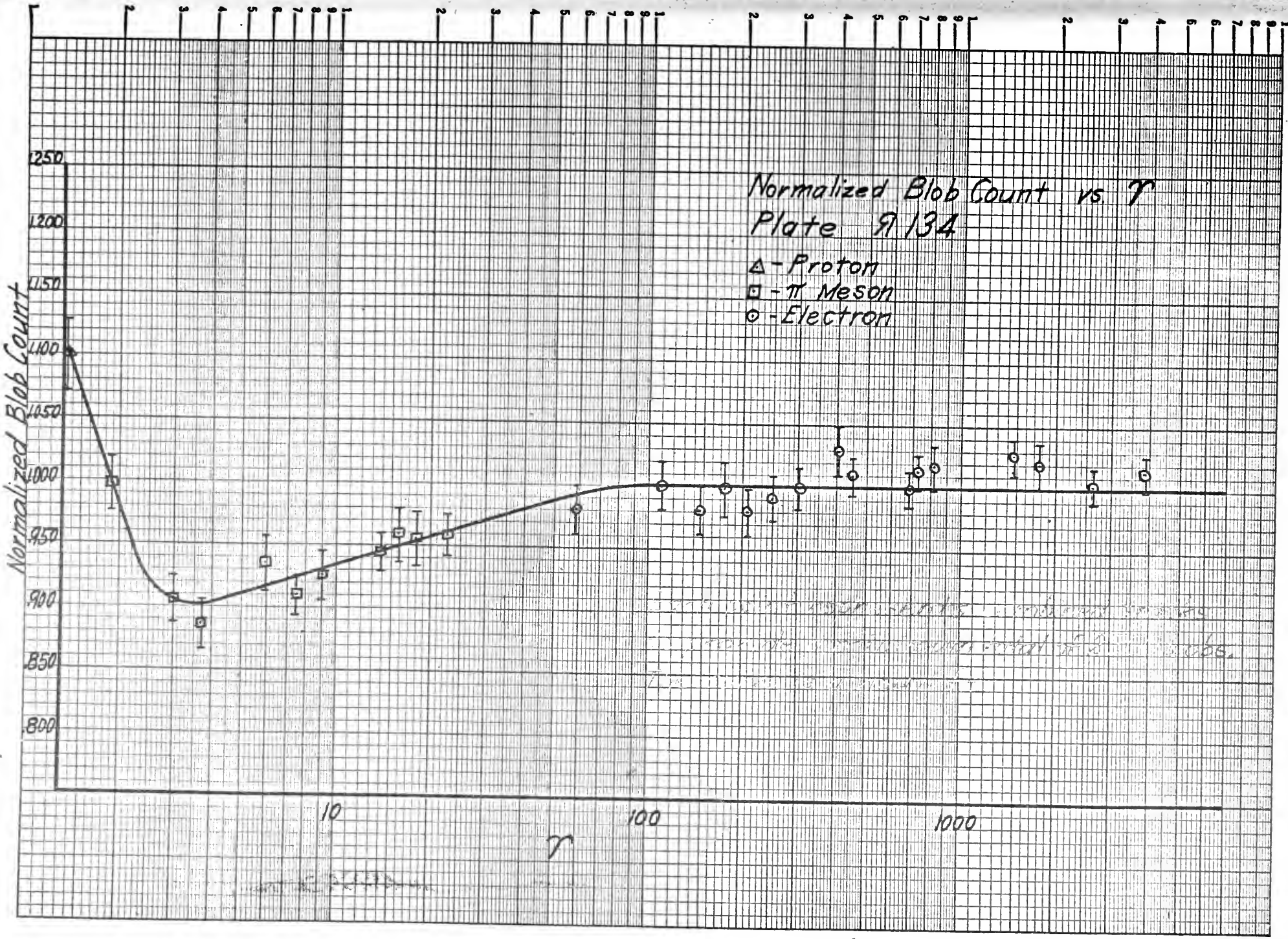
Normalized Blob Count vs γ
Plate 9134
Δ - Proton
□ - π Meson
○ - Electron
Normalized Blob Count
1250
1200
1150
1100
1050
1000
950
900
850
800
10
100
1000
γ

6. Comparison with theory and other experiments

As was described in Subhead 1, the relativistic rise to plateau has been investigated by many persons. In 1950, Pickup and Voyvodic /11/ reported indications of a relativistic increase in grain density of about 10% to a plateau starting at $\gamma \cong 20$. Similar results were obtained by Daniel et al /15/. In 1953 Stiller and Shapiro /17/ reported a 14 $\pm$ 3% rise to plateau. In our experiment, as in Stiller and Shapiro's, blob densities were substituted for grain densities to simplify counting and facilitate reproducibility among observers. The magnitude of the relativistic rise of blob count determined was 14 $\pm$ 2% in our experiment.

The rate of rise to the plateau and the constant value on plateau indicated by our results is essentially the same as that determined by Stiller and Shapiro and many others but extends the investigated region on the plateau to higher values of γ. The effect noted by Alekseyeva et al /27/ was not observed.

Our data are entirely consistent with the theory as determined by Halpern-Hall /7/, and Sternheimer /9/, with the plateau beginning at γ greater than 100. This indicates a deviation from the theories of Daniel et al /15/ and Morrish /14/ which predict a plateau beginning about $\gamma = 20$.

7. Critique

Although the data seem to be in good agreement with currently accepted theory, there are possible sources of error which could obscure a departure from a flat plateau of ionization loss. These are the determination of γ from multiple scattering measurements and the variation of blob density with depth in the emulsion.

To check for systematic errors in our scattering data, the pellicles were taken to the Lawrence Radiation Laboratory at Berkeley and a random sample of tracks was scattered on the Koristka MS-2 belonging to the Barkas group. Consistent agreement within statistical error was found, and we consider this the best evidence we have for thinking that our estimates of γ are not systematically in error.

Since our data were insufficient to allow restricting all tracks to a small fraction of the emulsion thickness, a correction was required to compensate for the variation of blob density with depth. (See subhead 4.) Although pains were taken in the normalization, one must recognize that the variation with depth is a severe handicap. Some encouragement comes, however, from the consistent results obtained from pellicles with rather different normalizing curves.

APPENDIX I

SCATTERING PROGRAM

This program was written for the purpose of calculating the pv of a singly charged particle in a nuclear emulsion. The method of multiple scattering is described in the section on determination of velocity. Our program was written in Fortran 60 for specific use on a Control Data Corporation 1604 computer. A disadvantage for use as a general scattering program is that in order to compute an equivalent cell length, an estimate of v/c must be made. The data printout format was designed so that the actual computer paper could be filed and kept as a record. During the course of the experiment, printouts were added when deemed advantageous; until in its final form, the program outputs sufficient data to analyze the run.

The following are the program inputs. On the first card of each run:

Columns 1-3 Pellicle number

Columns 5-7 Event number

Columns 9-10 Prong number

*Column 11 Scanner identification

Columns 12-17 Date of scattering

Columns 18-22 Primary cell length

Columns 23-25 Number of Y coordinate readings

Columns 26-30 Estimate of v/c

Columns 31-35 Microscope calibration

* This number is used for filing and for choosing a personal noise reading written into the program.

On the second card of each run are the following:

Column 1 Number one if final track for this computer run; otherwise number zero.

Column 2 Number one if computer is to calculate pv with both calculated and personal noise; otherwise number zero.

Column 3 Always zero.

On the following data cards there are eight coordinate readings to each card, one reading every ten columns.

After reading the input cards, the computer calculates a noise reading; and using this noise reading, a value of pv. After a first run the program selects the personal noise reading for the individual doing the scattering, returns to the beginning, and re-calculates pv using this personal noise reading. The personal scanner noise was determined by having each person scatter the 16.2 Bev pions of the primary beam. Cell lengths of 100, 250, and 500 microns were used to scatter the pions; and since at these cell lengths the signal from a 16.2 Bev particle is virtually non-existent, any reading is noise. Enough tracks were scattered by each person to determine a mean value of individual noise. The

noise determined by this method was found to be independent of the cell length used.

The program outputs were selected so that crosschecks could be made. The outputs were:

1. The number of Y coordinate readings.
2. The Y coordinate readings.
3. All calculated second and third differences--if a second or third difference was cast out by the guillotine method, the corresponding second or third difference will print out as zero.
4. Number of readings cast out by the guillotine method--This output, together with output 3, can sometimes pinpoint a bremsstrahlung along an electron track.
5. Mean second and third differences--The calculation of second and third differences is made for primary cell lengths, double overlapping cell lengths, and triple overlapping cell lengths. There are six corresponding values of mean differences and cast outs.
6. The three calculated values of noise--Noise was calculated using primary and double cell lengths, primary and triple cell lengths, and double and triple cell lengths. Only the first value was used to compute pv, but the other two were printed out as a consistency check.

7. The actual second difference signal--This value is the square root of the mean second difference squared using primary cell lengths minus the calculated noise squared using primary and double cell lengths.
8. The signal using the mean third difference and the ratio of outputs 7 and 8.
9. The three values of pv (using the three mean second differences), the estimated statistical error, and the signal to noise ratio, all using calculated noise.
10. The three values of pv, the estimated statistical error, and the signal to noise ratio, all using personal scanner noise--If outputs 9 and 10 did not agree within the estimated statistical error, the track was either rescattered or discarded.
11. The mean second differences for primary cell lengths divided into segments of ten consecutive second differences--This output was found to give the best indication of a bremsstrahlung along an electron track. A bremsstrahlung can be suspected when the mean second difference increases to a higher value between successive segments, and then remains at this higher value in succeeding segments.

There is one noteworthy aspect to this program. In some situations the calculated noise can be a negative number. Since

this situation has no physical significance, the calculated noise is set equal to zero. When the computer is later asked for a ratio of signal to noise, it can be troublesome. This situation can be programmed out, or it can be handled as we did. When the calculated noise from primary and double cell lengths prints out as negative, the signal to calculated noise ratio is ignored--it is always infinite.

APPENDIX II

PROGRAM SCAT FLOW CHART

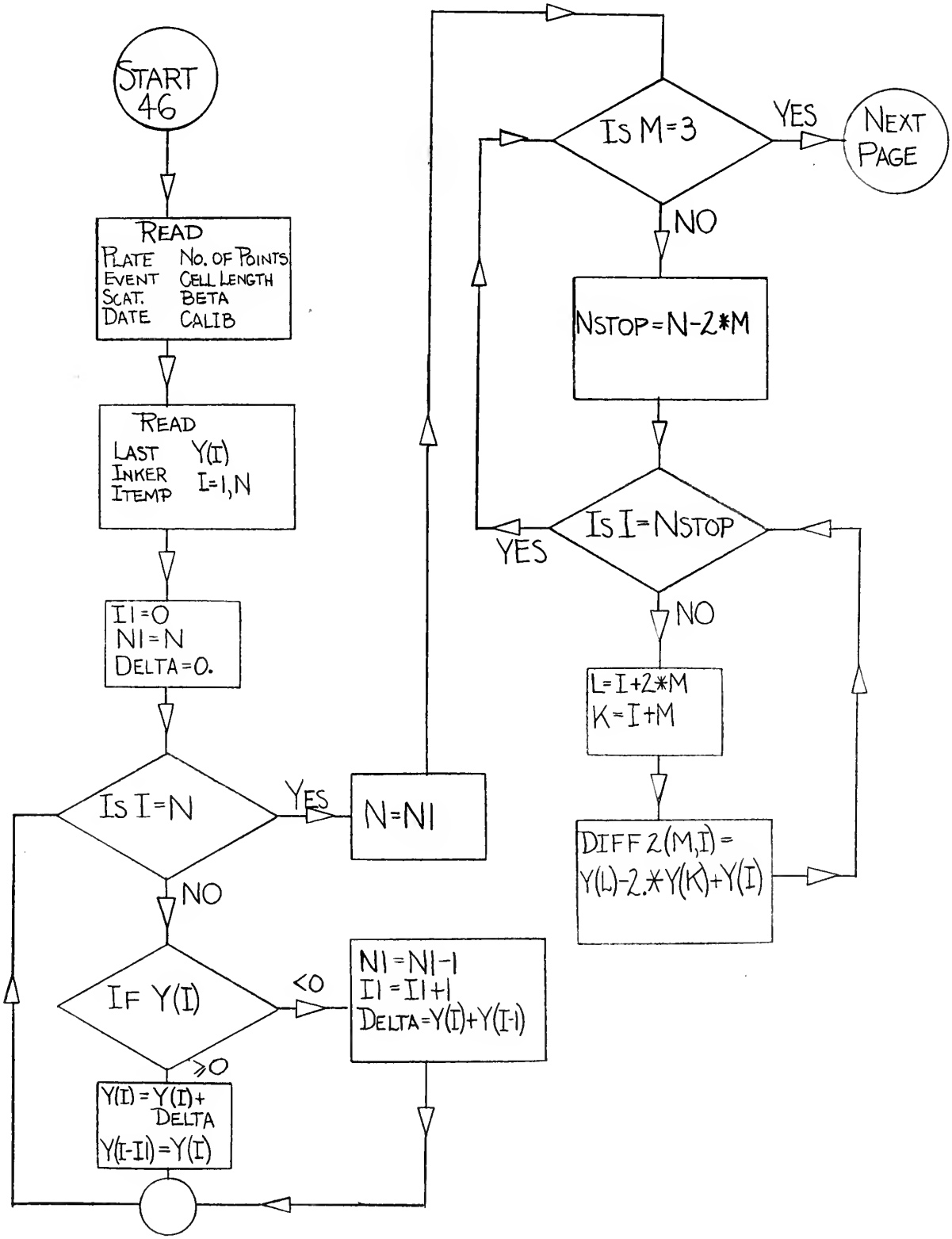

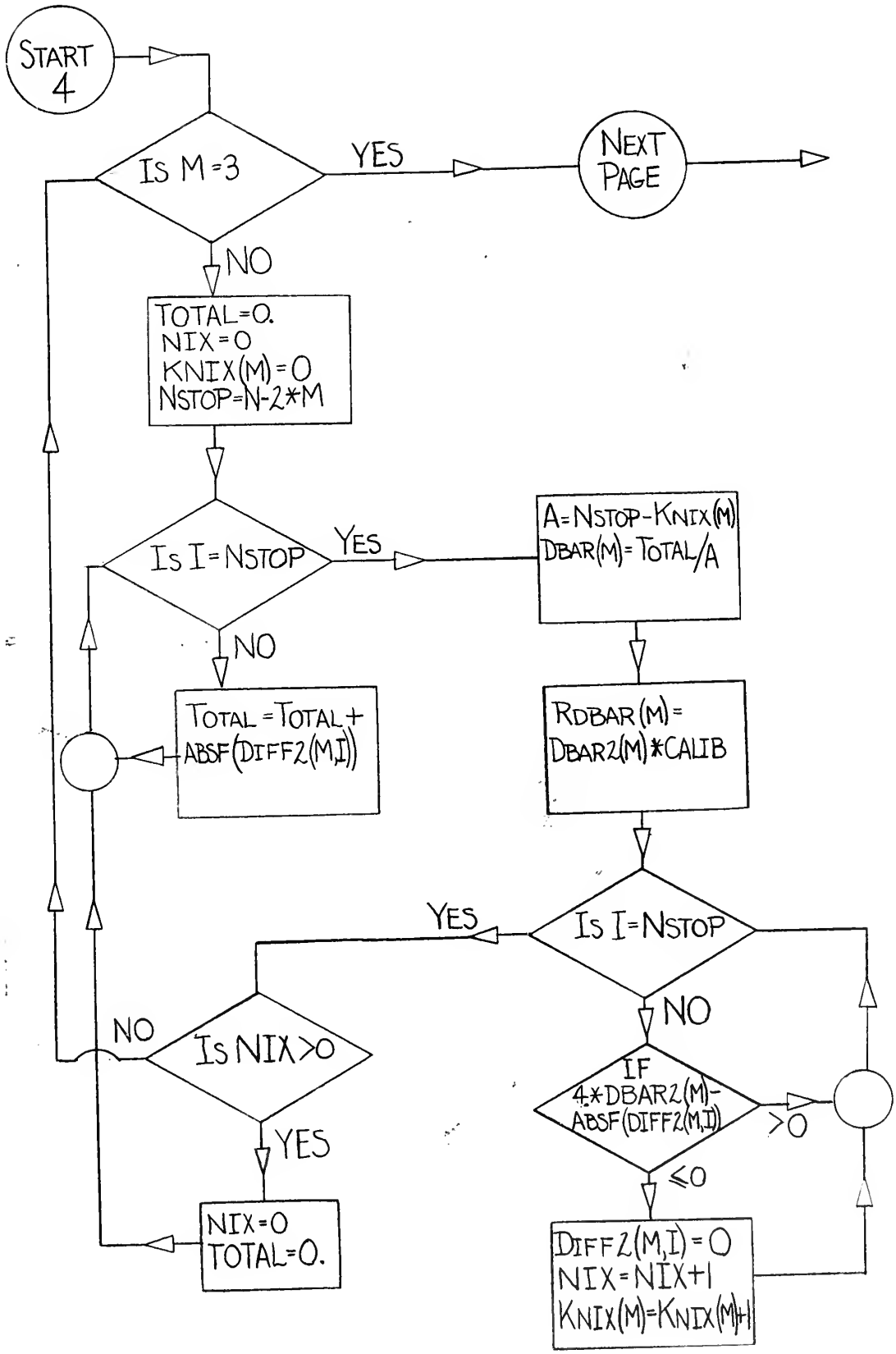
START 4
IS M=3
YES
NEXT PAGE
NO
TOTAL=0.
NIX=0
KNIX(M)=0
NSTOP=N-2*M
IS I=NSTOP
YES
A=NSTOP-KNIX(M)
DBAR(M)=TOTAL/A
NO
TOTAL=TOTAL+
ABSF(DIFF2(M,I))
RDBAR(M)=
DBAR2(M)*CALIB
IS I=NSTOP
YES
NO
IS NIX>0
NO
IF
4.*DBAR2(M)-
ABSF(DIFF2(M,I))
>0
≤0
YES
NIX=0
TOTAL=0.
DIFF2(M,I)=0
NIX=NIX+1
KNIX(M)=KNIX(M)+1

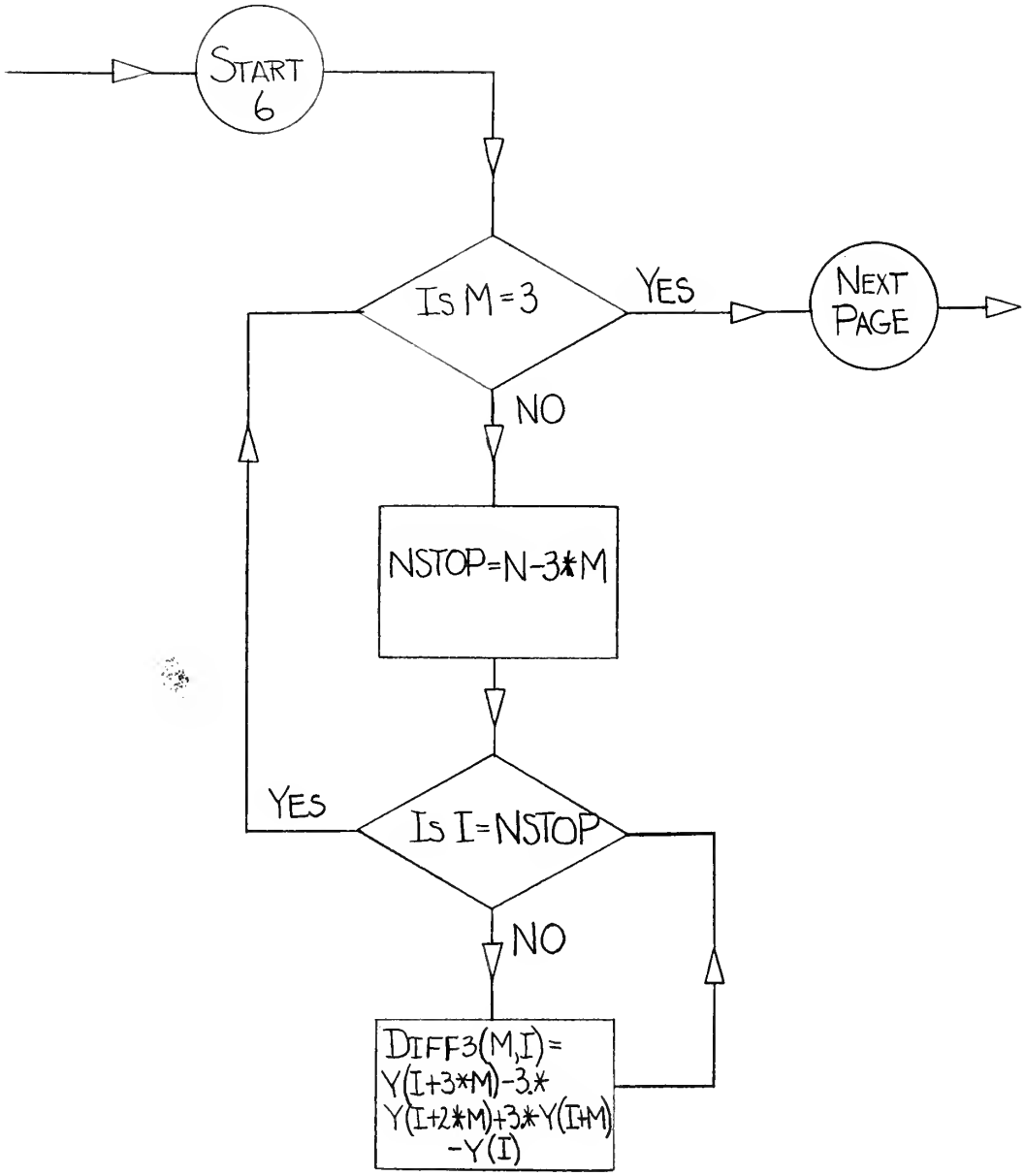
START
6
IS M=3
YES
NEXT
PAGE
NO
NSTOP=N-3*M
YES
IS I=NSTOP
NO
DIFF3(M,I)=
Y(I+3*M)-3.*
Y(I+2*M)+3.*Y(I+M)
-Y(I)

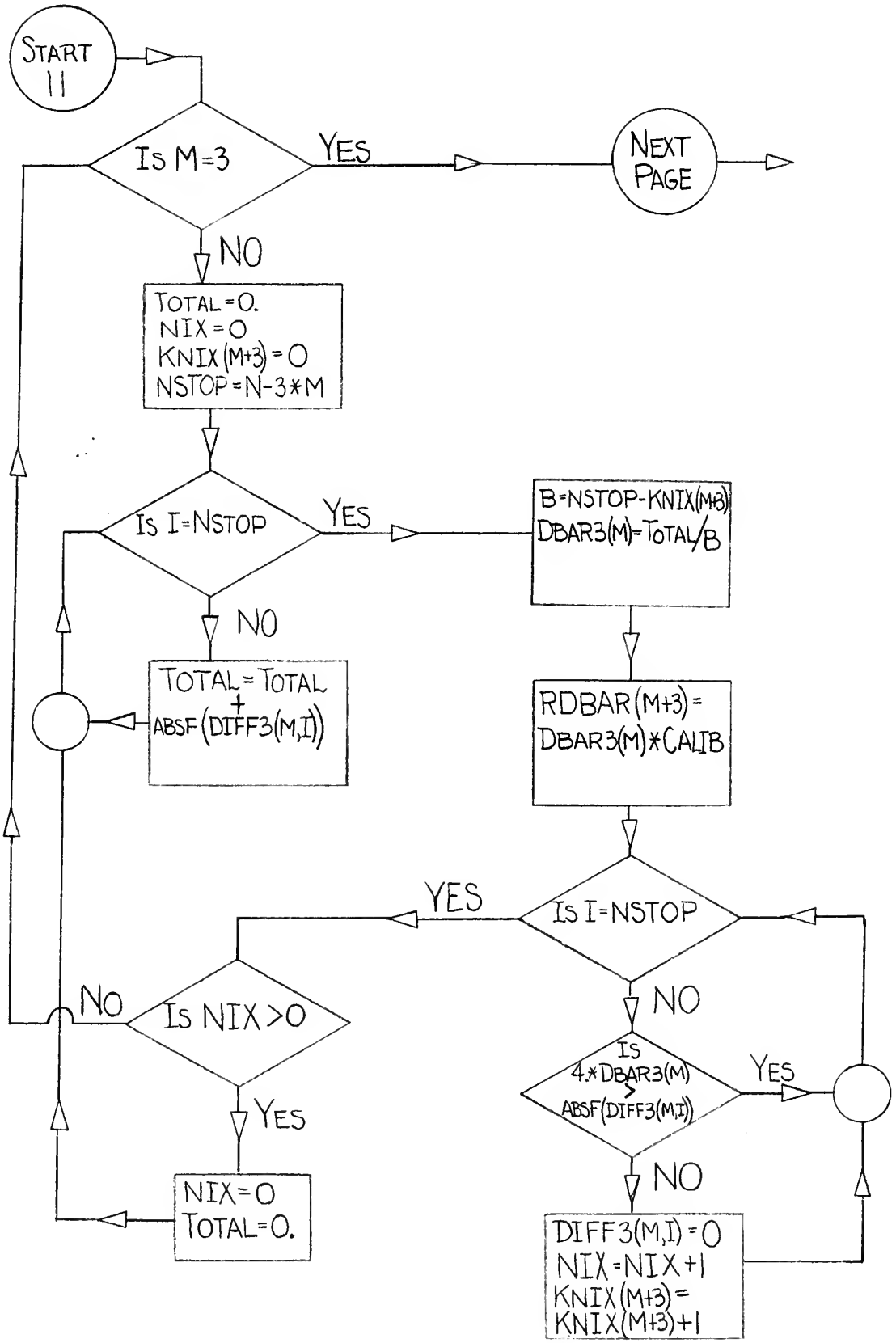
START
11
IS M=3
YES
NEXT
PAGE
NO
TOTAL=0.
NIX=0
KNIX(M+3)=0
NSTOP=N-3*M
IS I=NSTOP
YES
B=NSTOP-KNIX(M+3)
DBAR3(M)=TOTAL/B
NO
TOTAL=TOTAL
+
ABSF(DIFF3(M,I))
RDBAR(M+3)=
DBAR3(M)*CALIB
IS I=NSTOP
YES
NO
IS
4.*DBAR3(M)
>
ABSF(DIFF3(M,I))
YES
NO
DIFF3(M,I)=0
NIX=NIX+1
KNIX(M+3)=
KNIX(M+3)+1
IS NIX>0
NO
YES
NIX=0
TOTAL=0.

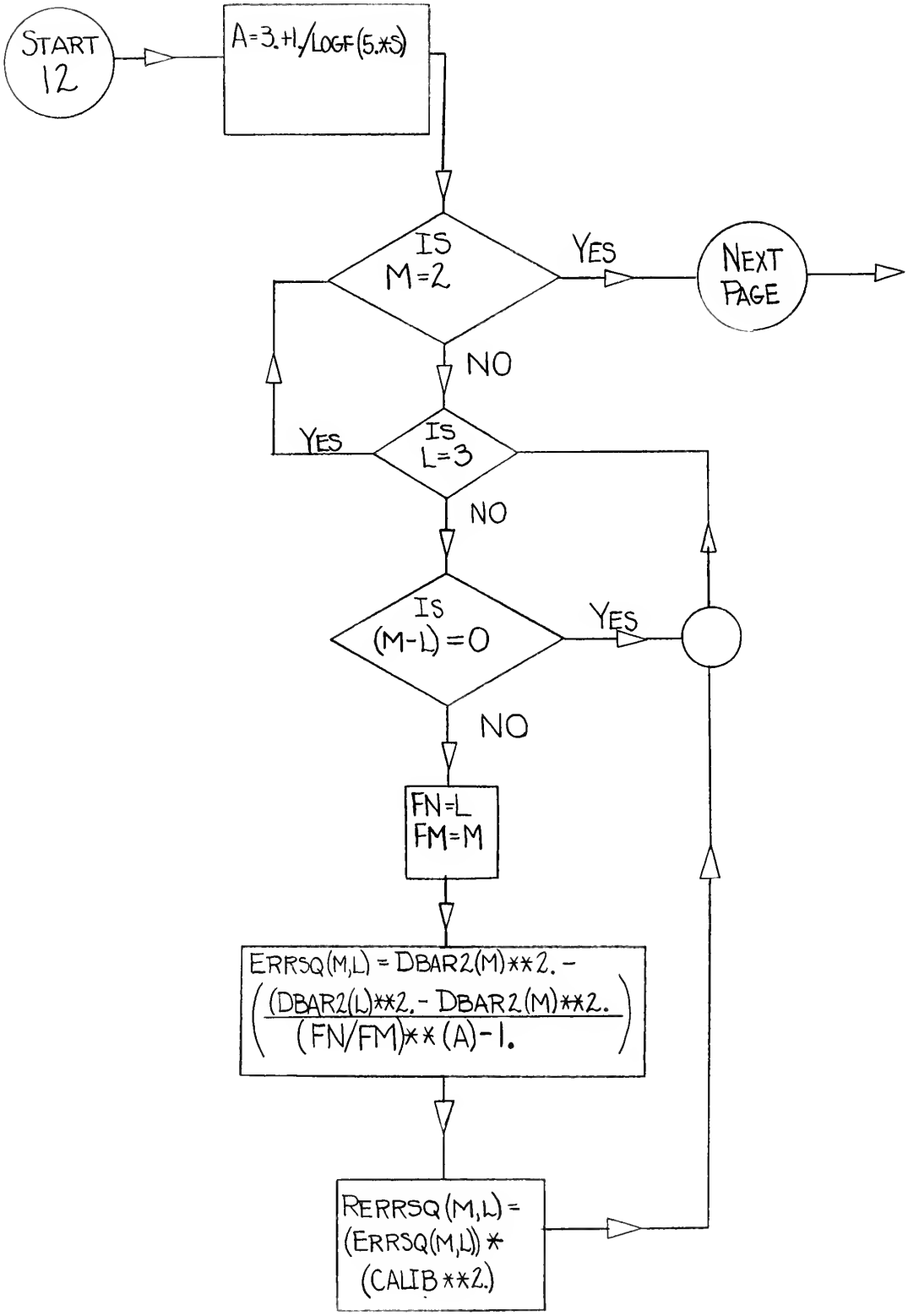
START
12
A=3.+1./LOGF(5.*S)
IS
M=2
YES
NEXT
PAGE
NO
YES
IS
L=3
NO
IS
(M-L)=0
YES
NO
FN=L
FM=M
ERRSQ(M,L) = DBAR2(M)**2. -
((DBAR2(L)**2. - DBAR2(M)**2.)
(FN/FM)**(A)-1.)
RERRSQ(M,L) =
(ERRSQ(M,L)) *
(CALIB**2.)

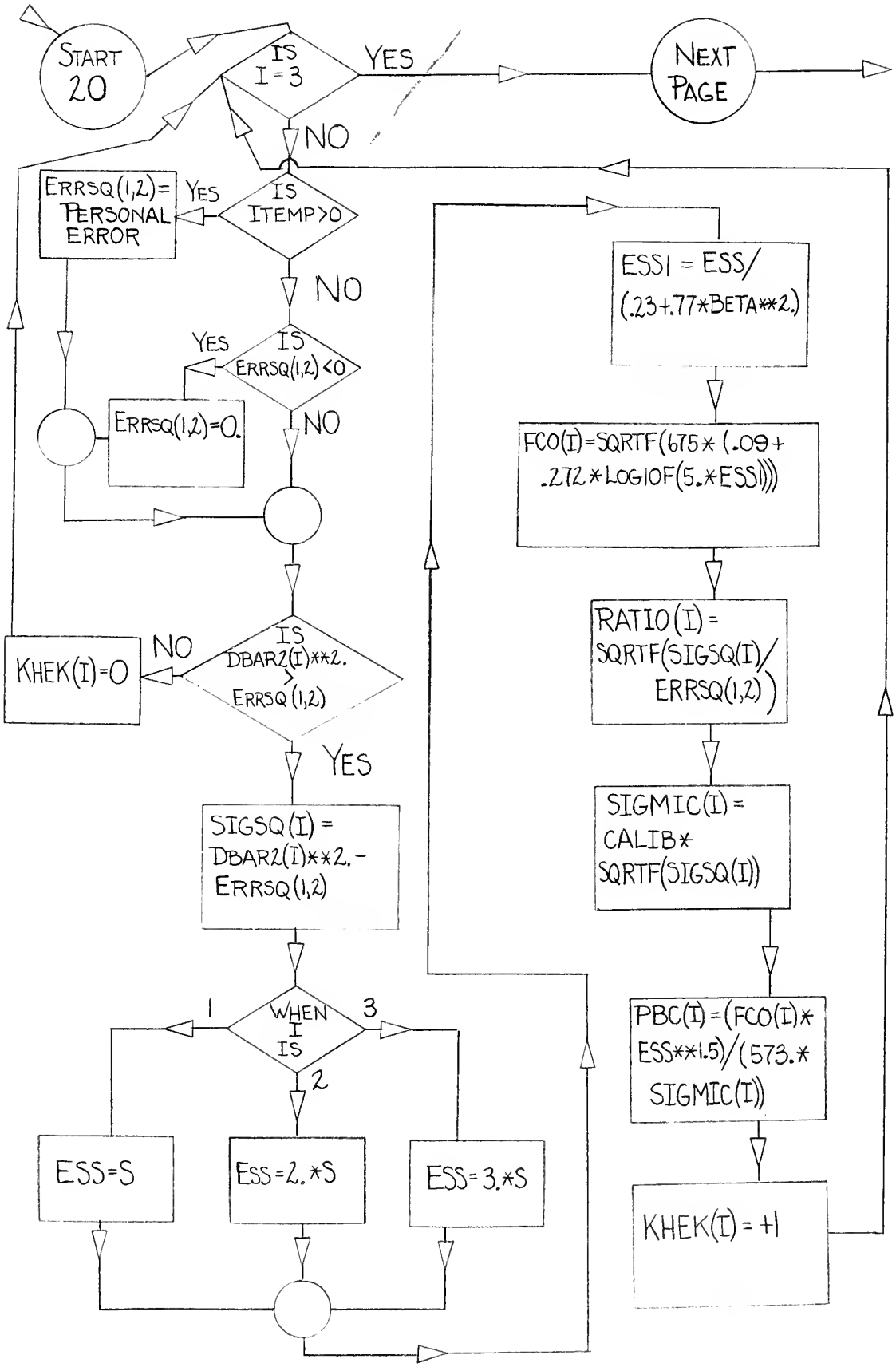
START 20
IS I = 3
YES
NEXT PAGE
NO
ERRSQ(1,2) = PERSONAL ERROR
YES
IS ITEMP > 0
NO
YES
IS ERRSQ(1,2) < 0
ERRSQ(1,2) = 0.
NO
KHEK(I) = 0
NO
IS DBAR2(I)**2. > ERRSQ(1,2)
YES
SIGSQ(I) = DBAR2(I)**2. - ERRSQ(1,2)
WHEN I IS
1
2
3
ESS = S
ESS = 2.*S
ESS = 3.*S
ESS1 = ESS/ (.23+.77*BETA**2.)
FCO(I) = SQRTF(675*(.09+ .272*LOG10F(5.*ESS1)))
RATIO(I) = SQRTF(SIGSQ(I)/ ERRSQ(1,2))
SIGMIC(I) = CALIB* SQRTF(SIGSQ(I))
PBC(I) = (FCO(I)* ESS**1.5)/(573.* SIGMIC(I))
KHEK(I) = +1

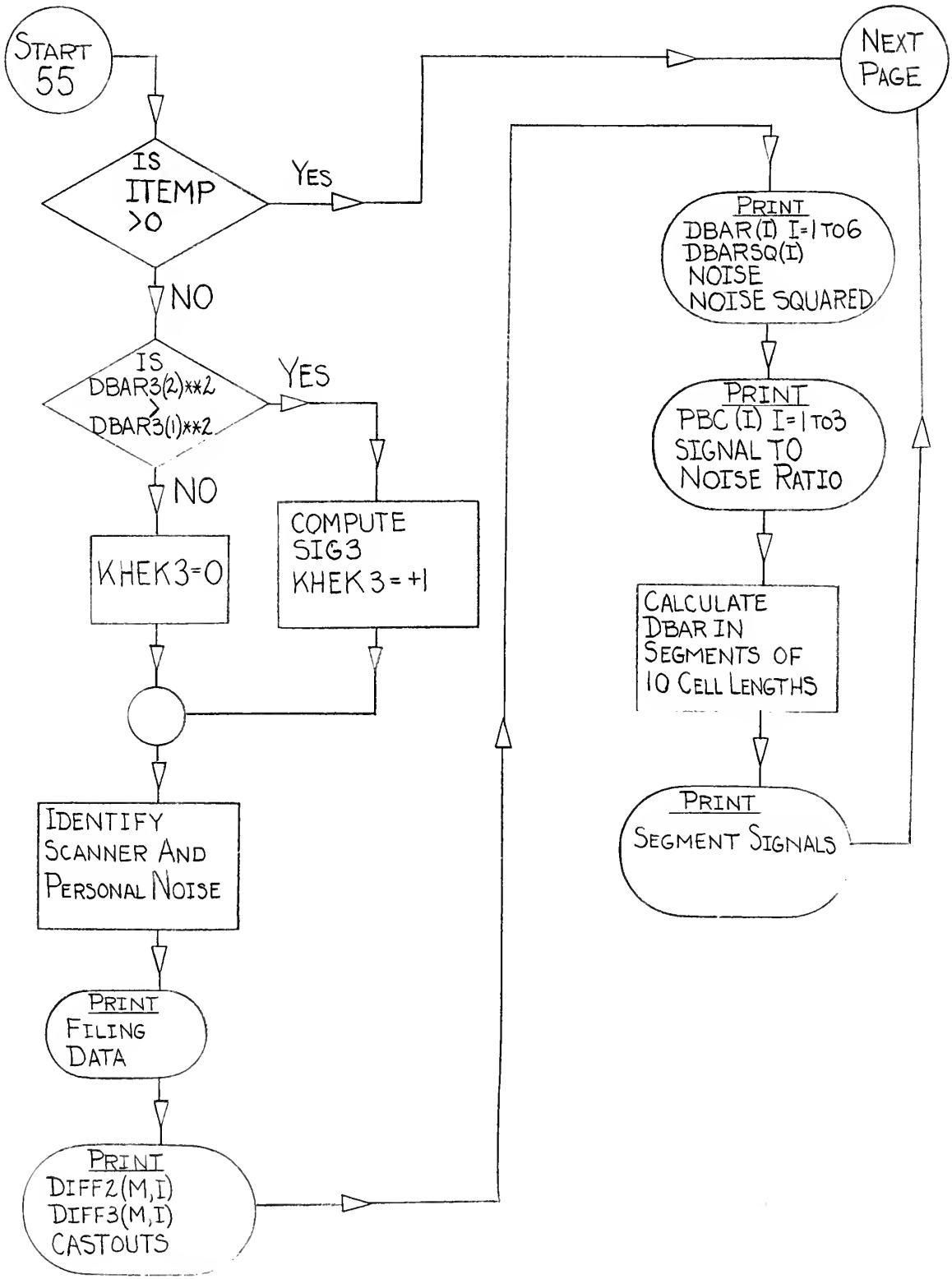
START 55
IS ITEMP >0
YES
NO
IS DBAR3(2)**2 > DBAR3(1)**2
YES
NO
KHEK3=0
COMPUTE SIG3
KHEK3=+1
IDENTIFY SCANNER AND PERSONAL NOISE
PRINT FILING DATA
PRINT DIFF2(M,I) DIFF3(M,I) CASTOUTS
NEXT PAGE
PRINT DBAR(I) I=1 TO 6 DBARSQ(I) NOISE NOISE SQUARED
PRINT PBC(I) I=1 TO 3 SIGNAL TO NOISE RATIO
CALCULATE DBAR IN SEGMENTS OF 10 CELL LENGTHS
PRINT SEGMENT SIGNALS

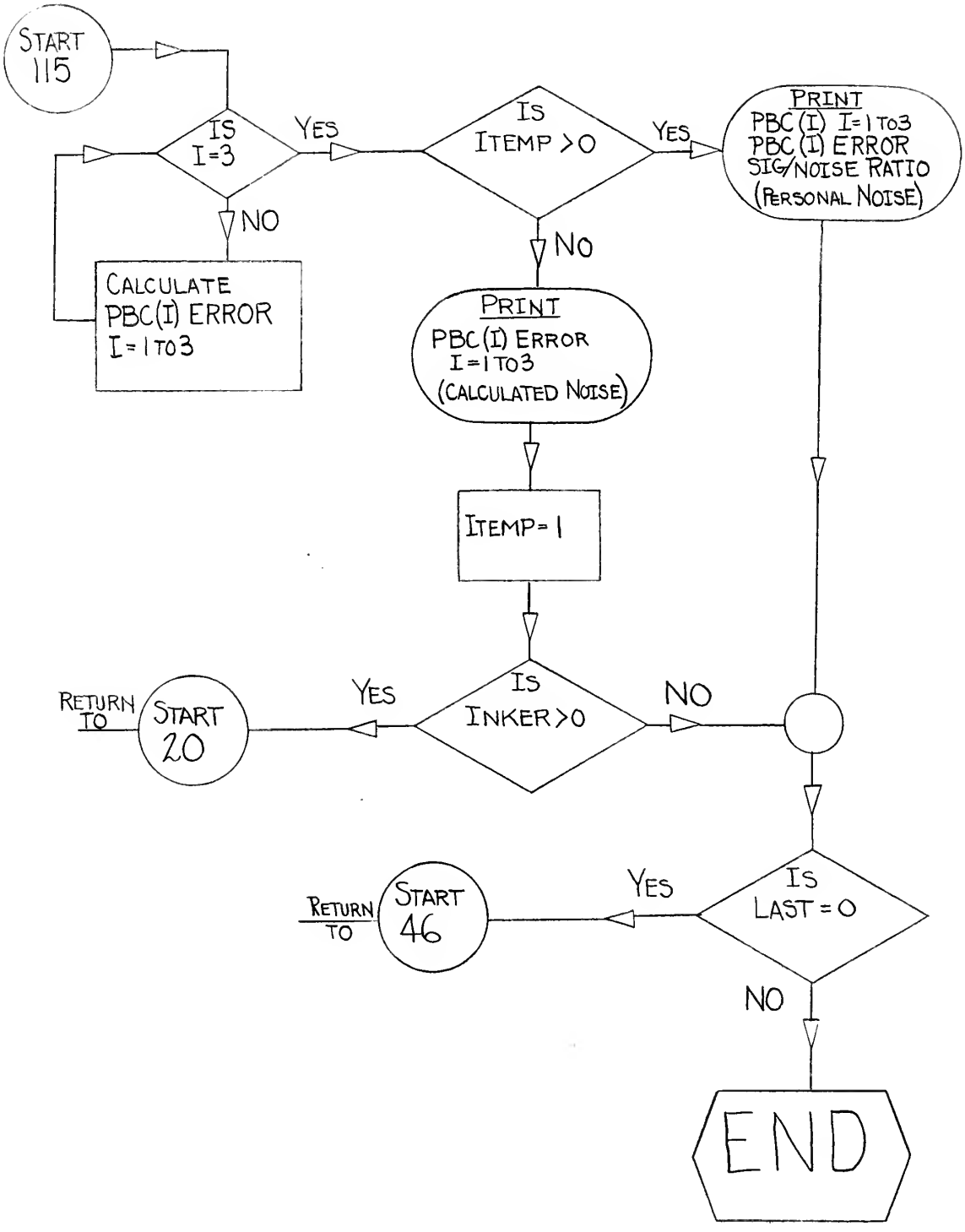
START 115
IS I=3
YES
NO
CALCULATE PBC(I) ERROR I=1 TO 3
IS ITEMP >0
YES
No
PRINT PBC(I) I=1 TO 3 PBC(I) ERROR SIG/NOISE RATIO (PERSONAL NOISE)
PRINT PBC(I) ERROR I=1 TO 3 (CALCULATED NOISE)
ITEMP=1
IS INKER>0
YES
NO
RETURN TO START 20
IS LAST=0
YES
NO
RETURN TO START 46
END

PROGRAM LISTING

```
      PROGRAM SCAT
C          PROGRAM SCAT          SYMBOL DEFINITIONS
C     IDEV    FIRST 3, PELL NBR    2ND 3, STAR NBR, LAST 2, PRONG NBR
C     IDSC    SCANNER  NUMBER
C     IDATE   MONTH, DAY, YEAR  DATA TAKEN
C     S       CELL LENGTH IN MICRONS
C     N       NUMBER OF READINGS IN EVENT
C     BETA    ESTIMATED BETA AT INPUT
C     LAST    NON-ZERO FOR LAST EVENT IN RUN
C     Y(I)    ORDINATES IN MICROMETER UNITS
C     DIFF2(M,I)  IS   I-TH  2ND DIFF FOR CELL LENGTH MS
C     DIFF3(M,I)  IS   I-TH  3RD DIFF FOR CELL LENGTH MS
C     DBAR2(M)    IS MEAN 2ND DIFF FOR CELLS MS, WITH CUT-OFF
C     DBAR3(M)    IS MEAN 3RD DIFF FOR CELLS MS, WITHOUT CUT-OFF
C     SIGSQ(N)    IS SQUARE OF NOISE CORRECTED SEC DIFF FOR CELL NS,
C                    USING NOISE FROM SINGLE AND DOUBLE CELLS
C     ESS1    IS EFFECTIVE S FOR CALC OF  KCO
C     FCO(N) IS KCO  FOR CELL NS, IN FLT PT
C     KHEK(N)   +1 IF PBC CALC FOR CELL NS
C                0 IF NG BECAUSE NOISE GREATER THAN SIGNAL
C               -1 IF NG BECAUSE SIG LESS THAN  2 X NOISE
C     KHEK3   +1 IF 3RD DIFF CALC OK, 0 IF REJECTED
   46 PRINT 47
   47 FORMAT (9H1J.N.DYER //)
      DIMENSION Y(200),KNIX(6),DIFF2(3,198),DIFF3(3,198),DBAR2(3),
     1DBAR3(3),ERRSQ(3,3),SIGSQ(3),FCO(3),KHEK(3),RDBAR(6),RERRSQ(3,3),
     2SIGMIC(3),PBC(3),RBARS2(3),RATIO(3),
     3SEG(20)
C                 READ  IN  DATA
    1 FORMAT(I10, I1, I6, F5.0, I3, F5.3, F5.3)
    2 FORMAT(8F10.0)
    3 FORMAT (I1,I1,I1)
      READ 1, IDEV, IDSC, IDATE, S, N, BETA, CALIB
      READ 3, LAST, INKER, ITEMP
      READ 2, (Y(I),I=1,N)

C     REARRANGE FOR POSSIBLE DUPLICATES
      I1=0
      N1=N
      DELTA=0.
      DO 3000  I=1,N
      IF (Y(I)) 3002,3001,3001
 3001 Y(I) =Y(I)+ DELTA
      Y(I-I1) = Y(I)
      GO TO 3000
 3002 N1= N1-1
      I1= I1+1
      DELTA = Y(I) + Y(I-1)
 3000 CONTINUE
      N=N1
C                 CALCULATE SECOND DIFFERENCES
      DO 4   M=1,3
      NSTOP = N-2*M
      DO 5   I=1,NSTOP
      L = I+2*M
      K = I+M
      DIFF2(M,I) = Y(L)-2.*Y(K)+Y(I)
    5 CONTINUE
    4 CONTINUE
```

```
                CALCULATE MEAN SECOND DIFFERENCES WITH
                CUTOFF AT  4  DBAR
      DO 6  M=1,3
      TOTAL = 0.
      NIX = 0
      KNIX(M) = 0
      NSTOP = N-2*M
  102 DO 7 I= 1,NSTOP
      TOTAL = TOTAL + ABSF(DIFF2(M,I))
    7 CONTINUE
      A = NSTOP - KNIX(M)
      DBAR2(M) = TOTAL/A
      RDBAR(M)=DBAR2(M)*CALIB
      DO 8  I= 1,NSTOP
      IF (4.*DBAR2(M)-ABSF(DIFF2(M,I))) 9,9,8
    9 DIFF2(M,I) = 0.
      NIX = NIX+1
      KNIX(M) = KNIX(M)+1
    8 CONTINUE
  100 IF (NIX) 6,6,101
  101 NIX = 0
      TOTAL = 0.
      GO TO 102
    6 CONTINUE
                CALC  3RD  DIFFS
      DO 11 M=1,3
      NSTOP= N-3*M
      DO 10 I= 1,NSTOP
      DIFF3(M,I)=Y(I+3*M)-3.*Y(I+2*M)+3.*Y(I+M)-Y(I)
   10 CONTINUE
   11 CONTINUE
          CALCULATE MEAN THIRD DIFFERENCES WITH
                CUTOFF AT 4  DBAR
      DO 12 M=1,3
      TOTAL=0.
      NIX=0
      KNIX (M+3)=0
      NSTOP= N-3*M
   17 DO 13 I=1,NSTOP
      TOTAL= TOTAL + ABSF(DIFF3(M,I))
   13 CONTINUE
      B= NSTOP- KNIX(M+3)
      DBAR3(M)= TOTAL/B
      RDBAR(M+3)=DBAR3(M)*CALIB
      DO 14 I=1,NSTOP
      IF (4.*DBAR3(M)-ABSF(DIFF3(M,I))) 15,15,14
   15 DIFF3(M,I)=0.
      NIX=NIX+1
      KNIX(M+3)=KNIX(M+3)+1
   14 CONTINUE
      IF (NIX) 12,12,16
   16 NIX =0
      TOTAL =0.
      GO TO 17
   12 CONTINUE
                    CALCULATE NOISE SQUARED
      A = 3.+1./LOGF(5.*S)
      DO 20  M = 1,2
      DO 21  L = 2,3
      IF (M-L) 24,21,24
   24 FN = L
      FM = M
      ERRSQ(M,L)=DBAR2(M)**2.-((DBAR2(L)**2.-DBAR2(M)**2.)/((FN/FM)**A-
     1 1.))
      RERRSQ(M,L)=(ERRSQ(M,L))*(CALIB**2.)
   21 CONTINUE
   20 CONTINUE
```

```
                CALCULATE PBC FROM 1 AND 2 CELLS
                USING NOISE FROM 1 AND 2 CELLS
  22 DO 55 I=1,3
     IF(ITEMP) 122,122,1122
1122 ERRSQ (1,2)=PERSER
     GO TO 31
     ERRSQ(M,N) IS NOISE SQUARED FROM CELLS MS AND NS
 122 IF (ERRSQ(1,2)) 30,31,31
  30 ERRSQ(1,2) = 0.
  31 IF (DBAR2(I)**2. - ERRSQ(1,2)) 32,32,33
  33 SIGSQ(I) = DBAR2(I)**2. - ERRSQ(1,2)
     GO TO (341,340,34),I
 341 ESS = S
     GO TO 342
 340 ESS = 2.*S
     GO TO 342
  34 ESS=3.*S
 342 ESS1 = ESS/(.23 + .77*BETA**2.)
     FCO(I) =SQRTF(675.*(.09+.272*LOG10F(5.*ESS1)))
     SIGMIC(I) = CALIB*SQRTF(SIGSQ(I))
     PBC(I) = (FCO(I)*ESS**1.5)/(573.*SIGMIC(I))
     RATIO(I) = SQRTF(SIGSQ(I)/ERRSQ(1,2))
     KHEK(I) = +1
     GO TO 55
  32 KHEK(I) = 0
  55 CONTINUE
     IF(ITEMP) 2000,2000,2020
                     CALCULATE  SIGNAL FROM 3RD DIFFS
2000 IF(DBAR3(2)**2-DBAR3(1)**2) 200,200,201
 200 KHEK3 = 0
     GO TO 202
 201 SIG3 = SQRTF((DBAR3(2)**2.-DBAR3(1)**2.)/(1.5*((2.**A)-1.)))
     SIG3=SIG3*CALIB
     KHEK3= +1
 202 GO TO (60,61,63,64,66,67,69,70), IDSC
  60 ISCAN=8HJOHN
     GO TO 72
  61 ISCAN=8HFRED
     GO TO 72
  63 ISCAN=8HGAIL
     GO TO 72
  64 ISCAN=8HSHEILA
     GO TO 72
  66 ISCAN=8HHARRY
     GO TO 72
  67 ISCAN=8HRUSS
     PERSER =438.0745
     GO TO 72
  69 ISCAN=8HSWEDE
     PERSER =654.408
     GO TO 72
  70 ISCAN=8HDICK
     PERSER = 654.408
  72 PRINT 73
 730FORMAT (10X,10H EVENT NO.,10X,8HSCANNER , 10X,6H  DATE,10X,5H    S
    110X,3H  N)
     PRINT 74,IDEV,ISCAN,IDATE,S,N
  74 FORMAT (10X,I10,10X,A8,10X,I6,10X,F5.0,10X,I3 //)
     PRINT 75
 750FORMAT(15X,5H Y(I),8X,8H1DIF2(I),7X,8H2DIF2(I),7X,8H3DIF2(I),8X
    18H1DIF3(I),7X,8H2DIF3(I),7X,8H3DIF3(I))
     PLACE MATRIX IN HERE
     PRINT 76,Y(1)
  76 FORMAT (10X,F10.0)
     PRINT 77,Y(2),DIFF2(1,1)
  77 FORMAT(10X,F10.0,5X,F10.0)
     PRINT 78, Y(3),DIFF2(1,2),DIFF2(2,1),DIFF3(1,1)
  78 FORMAT(10X,F10.0,5X,F10.0,5X,F10.0,20X,F10.0)
     PRINT 79,Y(4),DIFF2(1,3),DIFF2(2,2),DIFF2(3,1),DIFF3(1,2),DIFF3(2,
    11)
  79 FORMAT(10XF10.0,5XF10.0,5XF10.0,5XF10.0,5XF10.0,5X,F10.0)
```

```
      K=N-9
      PRINT 85,(Y(I+4),DIFF2(1,I+3),DIFF2(2,I+2),DIFF2(3,I+1),
     1DIFF3(1,I+2),DIFF3(2,I+1),DIFF3(3,I),I=1,K)
   85 FORMAT(10XF10.0,5XF10.0,5XF10.0,5XF10.0,5XF10.0,5XF10.0,5XF10.0)
      K=N-7
      L=N-6
      PRINT 62,(Y(J+3),DIFF2(1,J+2),DIFF2(2,J+1),DIFF2(3,J),
     1DIFF3(1,J+1),DIFF3(2,J),J=K,L)
   62 FORMAT(10XF10.0,5XF10.0,5XF10.0,5XF10.0,5XF10.0,5XF10.0)
      K=N-4
      PRINT 65, Y(K+2),DIFF2(1,K+1),DIFF2(2,K),DIFF3(1,K)
   65 FORMAT(10XF10.0,5XF10.0,5XF10.0,20XF10.0)
      L=N-3
      PRINT 68, Y(L+2),DIFF2(1,L+1),DIFF3(1,L)
   68 FORMAT(10XF10.0,5XF10.0,35XF10.0)
      PRINT 71,Y(N)
   71 FORMAT (10X,F10.0)
      IAWAY=7HCASTOUT
      PRINT 80,IAWAY,KNIX(1),KNIX(2),KNIX(3),KNIX(4),KNIX(5),KNIX(6)
   80 FORMAT(10X,A7,14X,I3,12X,I3,12X,I3,12X,I3,12X,I3,12X,I3 ///)
      ISIG=6HSIGNAL
      IPBC=3HPBC
      IDBAR=4HDBAR
     OPRINT 86,IDBAR,DBAR2(1),DBAR2(2),DBAR2(3),DBAR3(1),DBAR3(2),
     1DBAR3(3)
  860FORMAT(10X,A4,11X,F10.2,5X,F10.2,5X,F10.2,5X,F10.2,5X,F10.2,5X
     1F10.2 /)
      PRINT 35,              RDBAR(1),RDBAR(2),RDBAR(3),RDBAR(4),RDBAR(5),
     1RDBAR(6)
   35 FORMAT (10X,7HDBARMIC,8X,F10.3,5X,F10.3,5X,F10.3,5X,F10.3,5X,
     1F10.3,5X,F10.3 /)
      INOISE=8HNOISE SQ
      IFIRST=5HM1 N2
      ISEC= 5HM1 N3
      ITHIRD=5HM2 N3
      DO 43 M=1,3
      RBARS2(M)=((DBAR2(M)*CALIB)**2.)
   43 CONTINUE
      JOY=8HDBARSQMI
      PRINT 44,JOY,RBARS2(1),RBARS2(2),RBARS2(3)
   44 FORMAT(10X,A8,5X,F10.5,5X,F10.5,5X,F10.5 ///)
  890PRINT 87,INOISE,IFIRST,ERRSQ(1,2),ISEC,ERRSQ(1,3),ITHIRD,
     1ERRSQ(2,3)
   87 FORMAT(10X,A8,5X,A5,2X,F10.3,5X,A5,2X,F10.3,5X,A5,2X,F10.3 /)
      ICHECK=6HNOISE
      JOY2=8HERRSQMIC
     OPRINT 45,JOY2,IFIRST,RERRSQ(1,2),ISEC,RERRSQ(1,3),ITHIRD,
     1RERRSQ(2,3)
   45 FORMAT(10X,A8,5X,A5,2X,F10.4,5X,A5,2X,F10.4,5X,A5,2X,F10.4 ///)
      DO 41 M=1,3
      IF (KHEK(M)) 97,98,97
   97 PRINT 3003,PBC(M),RATIO(M)
 3003 FORMAT(10X,3HPBC,10X,F10.1,24H   SIGNAL TO NOISE RATIO,F10.2 //)
      GO TO 41
   98 PRINT 42
   42 FORMAT (10X,3HPBC,10X,28HNOISE IS GREATER THAN SIGNAL //)
   41 CONTINUE
      LDIF=8HBY 3DIFF
      IF(KHEK3-0)92,92,90
   90 PRINT 91,ISIG  ,LDIF,SIG3
   91 FORMAT(10X,A6,A8,6X,F10.3 //)
      GO TO 94
   92 IBAD=4HBARF
      PRINT 93,ISIG  ,LDIF,IBAD
   93 FORMAT(10X,A6,A8,6X,A4 //)
   94 CONTINUE
      PRINT 120, SIGMIC(1)
  120 FORMAT (10X,15HSIGNAL BY 2DIFF,5X,F10.3 //)
      BUDGE = SIG3 / SIGMIC(1)
      PRINT 121, BUDGE
  121 FORMAT (10X,27HSIGNAL RATIO 3DIFF TO 2DIFF,F10.3 //)
```

```
                CALCULATE DBAR FROM SEGMENTS OF
                    10  DIFF2(1)
      TOTAL=0.
      KA     = 0
      MA = N-2
      MI=0
      DO 110 I=1,MA
      IF (DIFF 2 (1,I))  111,112,111
  111 TOTAL = TOTAL + ABSF(DIFF2(1,I))
      MI = MI +1
      IF ( MI - 10 ) 113,112,113
  113 IF (I - MA) 110,112,110
  112 IF (MI) 114,110,114
  114 KA = KA + 1
      B = MI
      SEG (KA) = TOTAL/B
      MI = 0
      TOTAL = 0.
  110 CONTINUE
                      CALC SIGNAL IN MICRONS FOR SEGMENTS
      DO 115 I=1,KA
      IF((SEG(I ))**2.-ERRSQ(1,2)) 116,116,117
  117 SEG(I)=(SQRTF((SEG(I))**2.-ERRSQ(1,2)))* CALIB
      GO TO 119
  116 SEG (I ) = 0.
  119 PRINT 118, SEG(I )
  118 FORMAT (10X,22HSEGMENT SIGNAL MICRONS,5X,F7.3 /)
  115 CONTINUE
                ESTIMATING ERROR IN PBC
 2020 DIMENSION PBCER(3)
      PRIM=N
      DO 400 I=1,3
      TEMP = KMIX(I)
      FL = I
      FACT1 = 1.+.022*(FL-1.)
      FACT2 = PRIM - (2.*FL+TEMP)
      DENOM = SQRTF(FACT1*FACT2/FL)
      PBCER(I) = PBC(I)*1.37/DENOM
  400 CONTINUE
      IF(ITEMP)402,402,2030
  402 PRINT 403
  403 FORMAT(10X,45HERROR IN MEV CALCULATED FROM PG264 CERN NOTES/)
      DO 406 J =1,3
      PRINT 404, PBCER(J)
  404 FORMAT(10X,17HPBC PLUS OR MINUS5X,F10.3/)
  406 CONTINUE
      ITEMP=1
      IF (INKER) 18,18,22
 2030 PRINT 2031
 2031 FORMAT (10X,24HPBC USING PERSONAL NOISE/)
      DO 2033 I=1,3
      PRINT 2032, PBC(I), PBCER(I), RATIO(I)
 2032 FORMAT (10X, F5.0,10X, 13HPLUS OR MINUS 5X, F5.0,
     110X, 21HSIGNAL TO NOISE RATIO 5X, F5.2/)
 2033 CONTINUE
   18 IF (LAST) 48,46,48
   48 CONTINUE
  408 END
      END
```

Acknowledgements

We are grateful to Dr. John N. Dyer for his continuing advice and leadership. His knowledge and experience in the field of nuclear emulsions made this experiment possible. Dr. Fred R. Buskirk provided us with the necessary background and theoretical ability to begin and to sustain this combined effort.

Our thanks go to our scanners, Miss Sheila Flynn and Mrs. Gail Henderson, for their arduous and meticulous work in locating the pairs and counting several hundred thousand blobs.

Many valuable discussions were held with Dr. Harry E. Handler, who has contributed much to this work.

We are indebted to Dr. Walter H. Barkas of the Lawrence Radiation Laboratory, Berkeley, for the use of the plates from his emulsion stack and the loan of some of the scanning equipment used in this project.

The Koristka microscope was kindly furnished by Dr. Hofstadter at Stanford University.

BIBLIOGRAPHY

1. N. Bohr, Phil. Mag. 30, 581 (1915).

2. H. Bethe, Ann. Physik 5, 325 (1930).

3. F. Bloch, Ann. Physik 16, 285 (1933).

4. W. F. G. Swann, J. Franklin Inst. 226, 441 (1938).

5. E. Fermi, Phys. Rev. 56, 1242 (1939); 57, 485 (1940).

6. G. C. Wick, Ricerca sci. 11, 49 (1940); Nuovo cimento (9) 1, 302 (1943).

7. O. Halpern and H. Hall, Phys. Rev. 73, 477 (1948).

8. M. Schönberg, Nuovo cimento 9, 210, 372 (1952).

9. R. M. Sternheimer, Phys. Rev. 88, 851 (1952); 89, 1148 (1953); 91, 256 (1953); 103, 511 (1956).

10. B. T. Price, Reports on Progress in Physics Vol. XVIII, 52 (1955).

11. E. Pickup and L. Voyvodic, Phys. Rev. 80, 89 (1950).

12. D. R. Corson and M. R. Keck, Phys. Rev. 79, 209 (1950).

13. I. B. McDiarmid, Phys. Rev. 84, 851 (1951).

14. A. H. Morrish, Phil. Mag. 43, 533 (1952).

15. R. R. Daniel, J. H. Davies, J.H. Mulvey, and D. H. Perkins, Phil. Mag. 43, 753 (1952).

16. M. Shapiro and B. Stiller, Phys. Rev. 87, 682 (1952).

17. B. Stiller and M. Shapiro, Phys. Rev. 92, 735 (1953).

18. R. P. Michaelis and G. B. Violet, Phys. Rev. 90, 723 (1953).

19. J. R. Fleming and J. J. Lord, Phys. Rev. 92, 511 (1953).

20. G. Alexander and R. H. W. Johnston, Nuovo cimento, Series X, 5, 363 (1957).

21. B. Jongejans, Nuovo cimento 16, 625 (1960).

22. J. W. Patrick and W. H. Barkas, Nuovo cimento, Supp. No. 1, Series X, 23, 1 (1962).

23. P. Budini, Nuovo cimento 10, 236 (1953); 4, 23 (1956).

24. C. O'Ceallaigh, CERN Report, Document BS-11, Geneva (1954); Nuovo cimento Supp. 12, 412 (1954).

25. P. H. Fowler and D. H. Perkins, Phil. Mag. (7) 46, 587 (1955).

26. W. H. Barkas, Univ. Calif. Lawrence Radiation Lab. Report UCRL-9578 (1961).

27. K. I. Alekseyeva, G. B. Zhdanov, M. J. Tretyakova, V. N. Zytovitch, and M. N. Shcherbakova, Proceedings of the IV International Conference on Nuclear Photography, Munich, 1962, 558 (1963).

28. B. Stiller, Proceedings of the IV International Conference on Nuclear Photography, Munich, 1962, 542 (1963).

29. M. M. Shapiro, Handbuch der Physik, Vol. XLV, Nuclear Instrumentation II 342 (1958).

30. W. H. Barkas, Nuclear Research Emulsions (Academic Press, New York, 1963) Vol. I

31. W. T. Scott, Phys. Rev. 85, 245 (1952).

32. D. H. Perkins, CERN 63-3, Feb. 1963, p. 245.

33. J. N. Dyer, (private communication), United States Naval Postgraduate School, 1963.

34. J. W. Patrick and W. H. Barkas, Univ. Calif. Lawrence Radiation Lab. Report UCRL-9692 (1961).